

國立臺灣大學理學院大氣科學研究所



碩士論文

Graduate Institute of Atmospheric Sciences

College of Science

National Taiwan University

Master Thesis

從日變化尺度探討臺灣山區雲霧森林的水文氣候循環
及其特殊性

The uniqueness of the hydro-climatological cycle in Taiwan's
montane cloud-fog forests

古鎔與

Rong-Yu Gu

指導教授：羅敏輝 博士

Advisor: Min-Hui Lo, Ph.D.

中華民國 109 年 7 月

July, 2020

誌謝



這份研究集結許多老師們辛苦的觀測，也讓我更認識美麗的臺灣山林。謝謝羅老師的悉心帶領，讓我學習用不同的角度解決問題，收穫許多發想及樂趣！謝謝莊振義老師、黃倬英老師、張世杰老師、陳奕穎博士提供通量塔與森林生態的觀測資料，以及謝謝褚侯森博士、李明旭老師、謝正義老師、蘇世顥老師、賴彥任博士、大氣系的老師們提供專業的討論與建議。謝謝實驗室的出差夥伴們，辛苦地陪我一起上山收資料、架儀器，也謝謝林博雄老師實驗室的協助。謝謝我的家人、實驗室的成員們、LAI 同學們、B03 同學們、系排夥伴們、大氣系的好朋友們在研究上的支持與照顧。最後，謝謝棲蘭山神無盡的包容，未來請繼續多多指教！

摘要

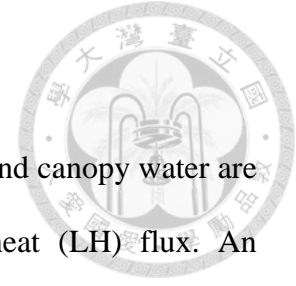


雲霧森林在一天之中經常有雲霧形成，過去研究多著重於定量霧對通量的抑制以及從水收支的角度分析雲霧森林的水文循環。經常性的雲霧是雲霧森林水文氣候重要的日尺度特徵，然而霧和地表通量日變化的關係卻較少被討論。我們從棲蘭的觀測發現不對稱的潛熱通量日變化，其峰值較太陽輻射的峰值提早約兩個小時，而在不會起霧的一般森林(以蓮華池森林為例)卻沒有這個現象。因此本研究欲從日變化尺度討論不對稱的潛熱通量如何反映兩地水文氣候的不同，以及其成因。透過比較棲蘭與蓮華池的觀測資料發現，棲蘭的潛熱通量峰值提早，會造成溫度的日變化幅度較小，配合谷風平流加上當地森林蒸發散量所導致的水氣累積，有利於在下午形成霧。雲霧可作為冠層水的來源，同時，棲蘭豐沛的雨量與夜晚潮濕的環境，使冠層水不易在夜晚蒸發而可維持潮濕至隔天清晨。早晨時，太陽輻射將可觀的冠層水蒸發，造成棲蘭的潛熱通量具有峰值提早的特徵。

本研究強調雲霧森林獨特的水文氣候特徵，亦即霧與潛熱通量的相互關聯。不對稱的潛熱通量、較小幅度的溫度日變化、經常性的午後雲霧以及可觀的冠層水，形塑棲蘭獨特的水文氣候循環。可觀的冠層水在棲蘭扮演著影響陸地與大氣交互作用的重要媒介，而降雨型態、溫度、長波輻射可能是控制冠層水量的重要因子。當氣候變遷造成冠層水減少，可能使起霧頻率減小，並影響雲霧森林的水文氣候。雖然雲霧減少是否有利於森林生態系的生長仍有待研究，但對於雨水豐沛的棲蘭而言，霧從能量方面影響植物生長的效應可能比從水量方面顯著。

關鍵字：潛熱通量、冠層水、蒸發、雲霧森林、霧、日變化

ABSTRACT



In Taiwan's montane cloud-fog forest, frequent afternoon fog and canopy water are essential to regulate evapotranspiration, also known as latent heat (LH) flux. An asymmetric LH flux with the early peak at 9 a.m. is found in Chi-Lan (CL) montane cloud-fog forest, but this phenomenon cannot be seen in the non-cloud-fog forests (taken LienHuaChih (LHC) forest as an example) from flux tower datasets. Observational results show that the early peak of LH flux in CL may result in a slower increase in near-surface temperature. The small diurnal temperature range plus water vapor accumulation from valley wind and local evapotranspiration makes the air frequently saturated at about 3 p.m., thus favoring fog formation. Then, the canopy can intercept fog water in the afternoon. The wetness is allowed to sustain throughout the night due to high relative humidity, then evaporating the next morning. We further utilized the land surface model to demonstrate the critical role of canopy water in regulating LH flux. The sensitivity tests display that precipitation, temperature, and downward longwave radiation in the atmospheric forcing have positive impacts on the asymmetry of LH flux. In summary, the characteristics of the asymmetric LH flux, small diurnal temperature range, frequent fog occurrence, and sufficient canopy water comprise the unique hydro-climatological cycle in the montane cloud-fog forest.

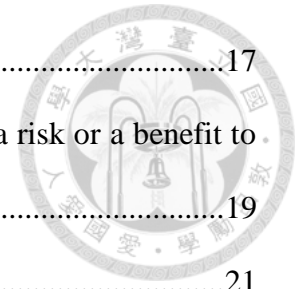
Keywords: latent heat flux, canopy water, canopy evaporation, cloud-fog forest, fog, diurnal analysis

CONTENTS

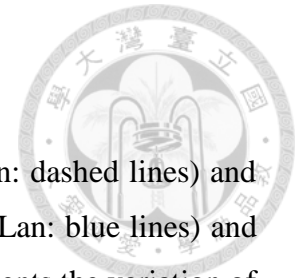


口試委員會審定書	#
誌謝	i
摘要	ii
ABSTRACT	iii
CONTENTS	iv
LIST OF FIGURES	vi
LIST OF TABLES	ix
Chapter 1 Introduction.....	1
Chapter 2 Data and Methodology.....	4
2.1 Site Description	4
2.2 Observational Datasets	6
2.2.1 Near-surface meteorological variables.....	6
2.2.2 Leaf Wetness Measurements	6
2.3 Model simulations	6
Chapter 3 Results.....	10
3.1 The impact of the asymmetric LH flux on the formation of the afternoon fog.....	10
3.2 The importance of canopy water to the asymmetric LH flux.....	11
3.3 Canopy water sensitivity test.....	12
3.4 The controlling factors to plentiful canopy water before sunrise.....	13
3.4.1 The setting of land surface or the atmospheric forcing?.....	13
3.4.2 Sensitivity test of the atmospheric forcing.....	14
Chapter 4 Discussion.....	16
4.1 The signal of the asymmetric LH flux.....	16
4.2 The sensitivity test of maximum allowed canopy water	16

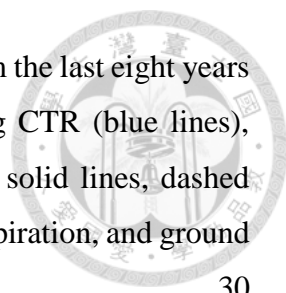
4.3	The drizzle's effect on the asymmetry of LH flux.....	17
4.4	The diurnal LH flux and the fog under climate change: a risk or a benefit to the ecosystem in CL?.....	19
4.5	The importance of fog description in models.....	21
Chapter 5	Conclusion	22
FIGURES	24
TABLES	40
REFERENCES	48



LIST OF FIGURES



- Figure 1.1** The comparison of the diurnal cycle of net radiation (Rn: dashed lines) and latent heat flux (LH flux: solid lines) between CL (Chi-Lan: blue lines) and LHC (LienHuaChih: red lines). The shading color represents the variation of the energy fluxes between the first quartile and the third quartile from four years of data from 2008 to 2011 in CL and two years of data from 2012 to 2013 in LHC.24
- Figure 2.1** The location of CL flux tower site (green triangle). (The figure is taken from Klemm et al. (2006).).....25
- Figure 2.2** The location of LHC flux tower site (red dot). (The figure is taken from Chen et al. (2012).).....26
- Figure 2.3** The land type comparison between CL and LHC and the measurements in CL. (The middle map in which green area represents the distribution of montane cloud-fog forests in Taiwan is taken from Schulz et al. (2017).).....27
- Figure 3.1** Five meteorological variables obtained from the flux towers in CL (blue lines) and LHC (red lines): (a) temperature, (b) specific humidity (solid lines) and saturated specific humidity (dashed lines), (c) wind speed, and (d) relative humidity. The shading color represents the variation of each meteorological variable between the first quartile and the third quartile from four years of data in CL and five years of data in LHC.28
- Figure 3.2** (a) Simulations conducted by the Community Land Model V4: with (CTR: blue lines) and without (EXP: orange lines) canopy water representation. (b) The comparison of the diurnal cycle of net radiation (dashed lines) and LH flux (solid lines) between CTR and EXP. (c) (d) The partition of LH flux (including ground evaporation (brown lines), transpiration (red lines), and canopy evaporation (blue lines)) for (c)CTR and (d)EXP. The shading color represents the variation of the energy fluxes between the first quartile and the third quartile from the last eight years of the simulations.29
- Figure 3.3** (a) The contribution of different source of water on the canopy, including fog (blue bars), rain (green bars) and dew (red bars). (b) The comparison of the diurnal cycle of LH flux among CTR (blue line), Rain+Dew (green line) and DEWonly (red line). The shading color represents the variation of the LH



fluxes between the first quartile and the third quartile from the last eight years of each simulation. (c) The partition of LH flux among CTR (blue lines), Rain+Dew (green lines) and DEWonly (red lines). The solid lines, dashed lines and dotted lines represent canopy evaporation, transpiration, and ground evaporation, respectively.30

Figure 3.4 (a) The comparison of the diurnal cycle of LH flux among CTR_3yr (blue line), LHCatm_CLsurf (red line) and CLatm_LHCsurf (green line). The shading color represents the variation of the LH fluxes between the first quartile and the third quartile from the last nine years of each simulation. (b) The partition of LH flux among CTR_3yr (blue lines), LHCatm_CLsurf (red lines) and CLatm_LHCsurf (green lines). The solid lines, dashed lines and dotted lines represent canopy evaporation, transpiration, and ground evaporation, respectively. (c) The comparison of the diurnal cycle of canopy water among CTR_3yr, LHCatm_CLsurf and CLatm_LHCsurf. The shading color represents the variation of the canopy water between the first quartile and the third quartile from the last nine years of each simulation.....31

Figure 3.5 Atmospheric forcing sensitivity test: comparing the proportion of the partition of LH flux including canopy evaporation (blue bars), transpiration (red bars) and ground evaporation (brown bars).....32

Figure 3.6 Atmospheric forcing sensitivity test: comparing (a) canopy evaporation and (b) canopy water in each sensitivity run with CTR_3yr and LHCatm_CLsurf.33

Figure 4.1 The comparison of the occurrence probability of the daily maximum LH flux between CL (blue line) and LHC (red line).....34

Figure 4.2 (a) The comparison of the diurnal cycle of canopy water among CTR (blue line), max_cw_0.2 (purple line) and max_cw_0.1 (dark magenta line) and max_cw_0.05 (light magenta line). The shading color represents the variation of the canopy water between the first quartile and the third quartile from the last eight years of each simulation. (b) The comparison of the diurnal cycle of LH fluxes among CTR, max_cw_0.2 and max_cw_0.1 and max_cw_0.05. The shading color represents the variation of the canopy water between the first quartile and the third quartile from the last eight years of each simulation. (c) The partition of LH flux among CTR, max_cw_0.2 and max_cw_0.1 and

max_cw_0.05. The solid lines, dashed lines and dotted lines represent canopy evaporation, transpiration, and ground evaporation, respectively.35

Figure 4.3 The comparison of probability density function (P.D.F.) in precipitation between CL (blue line) and LHC (red line).36

Figure 4.4 (a) The comparison of probability density function in precipitation between LHCatm_CLsurf (red line) and LHCatm_Clim_precip (orange line). (b) The comparison of the diurnal cycle of canopy water among LHCatm_CLsurf and LHCatm_Clim_precip The shading color represents the variation of the canopy water between the first quartile and the third quartile from the last nine years of each simulation. (c) The partition of LH flux among LHCatm_CLsurf and LHCatm_Clim_precip The solid lines, dashed lines and dotted lines represent canopy evaporation, transpiration, and ground evaporation, respectively. The shading color represents the variation of the canopy water between the first quartile and the third quartile from the last nine years of each simulation. (d) The comparison of the diurnal cycle of LH flux among LHCatm_CLsurf and LHCatm_Clim_precip The shading color represents the variation of the LH fluxes between the first quartile and the third quartile from the last nine years of each simulation.37

Figure 4.5 The effects of fog on (a) LH flux and (b) CO2 flux in CL montane cloud-fog forest. The solid dots represent the mean values of fluxes in foggy conditions in each time step, while the hollow dots represent those in fogless conditions. The solid line shows the averaged fluxes in foggy conditions from 6 a.m. to 6:30 p.m., while the dashed line shows those in fogless conditions from 6 a.m. to 6:30 p.m.38

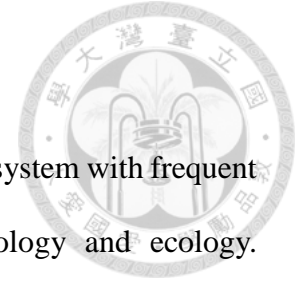
Figure 5.1 Schematic plot of the hydro-climatological cycle in CL montane cloud forest.39

LIST OF TABLES



Table 2.1 Experiment design: the contribution of canopy water on the LH flux.....	40
Table 2.2 Experiment design: canopy water sensitivity test	41
Table 2.3 Experiment design: the controlling factors to the asymmetric LH flux in CL (group 1)	42
Table 2.4 Experiment design: the controlling factors to the asymmetric LH flux in CL (group 2)	43
Table 3.1 The difference of leaf wetness between 6 a.m. and 9 a.m. in 3 different canopy layers. The positive mean value represents the canopy being wetter at 6 a.m. than at 9 a.m.....	45
Table 4.1 Experiment design: the sensitivity test of the maximum allowed canopy water	46
Table 4.2 Experiment design: the impact of drizzle on the asymmetry of LH flux.....	47

Chapter 1 Introduction



Montane cloud-fog forest, generally recognized as a forested ecosystem with frequent fog immersion in montane regions, is of great value to hydrology and ecology. Considerable cloud and fog droplets are set to become a vital factor in watershed yields and local biome growth, making the forest become a hotspot of species richness and biodiversity (Bruijnzeel et al., 2011; Bruijnzeel, 2001; Bubb et al., 2004; Goldsmith et al., 2013). Recently, such a unique ecosystem is facing a risk of fog disappearance. Anthropogenic forcing, such as rising temperature and elevated CO₂ concentration, may lift the cloud base height and influence water vapor supply from evapotranspiration, thus posing a threat to fog formation (Foster, 2001; Nair et al., 2003; Oliveira et al., 2014; Still et al., 1999; Williams et al., 2015).

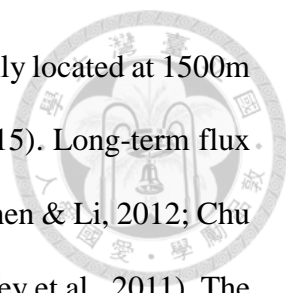
Fog can remarkably affect the hydro-climatology in the forest (Anber et al., 2015; Ataroff & Rada, 2000; Mildenerger et al., 2009). From the energy cycle perspective, fog can strongly block solar radiation, while diffused sunlight may increase due to better scattering ability of small water droplets (Anber et al., 2015; Lai et al., 2006). From the water cycle perspective, the wet environment can reduce the vapor pressure deficit. Intercepted by the canopy, fog water cannot be negligible from total water input to the ecosystem. The water may account for up to 30% of total precipitation, supporting foliar uptake for some vegetation, especially in some regular dry seasons (Limm et al., 2012). With the interception water above the stomata, transpiration is commonly reduced although some species can exceptionally maintain photosynthesis because of the xeromorphic traits on leaves (Chu et al., 2014; Goldsmith et al., 2013; Pariyar et al., 2017). After fog events, evaporation from the canopy water may happen if there is enough solar radiation. The evaporation from the soil is relatively insignificant in the montane cloud-

fog forest and used to be neglected from the water balance equation of LH flux (Klemm et al., 2006). To summarize, combining the energy and water perspective, there is a consensus of a total reduction of LH flux under foggy conditions (Chu et al., 2014; Goldsmith et al., 2013; Mildenberger et al., 2009).

Among all the cloud-fog forests, the characteristics of hydro-climatology in perhumid montane cloud-fog forest can be much more different. In the perhumid forest characterized by upslope fog, the amount of annual precipitation is twice more than that in typical forests, but the annual LH flux is half less (Bruijnzeel et al., 2011; Chu et al., 2014; Oliveira et al., 2014). Plentiful precipitation can serve as a source of canopy water, making the forest seldom suffer from moisture limitation. Besides, the canopy water usually can last longer on the leaves comparing to the duration of each fog and rain events in this foggy and wet environment. Therefore, canopy evaporation is expected to be a major contributor to LH flux (Chu et al., 2014; Giambelluca et al., 2009). Once the water vapor exchange from the land to the atmosphere, it cools near-surface temperature and moistens the boundary layer. The time scale of canopy evaporation is within one day, which is the shortest response among the other components (transpiration and soil evaporation) in the total LH flux (Wang et al., 2006).

Since the recurring fog also happens in daily timescale, high canopy evaporation in the perhumid montane cloud forest is expected to impact the fog climatology. Previous field studies were mostly done with intensive observation and used to focus on quantifying fog interception and the unidirectional effects of fog on LH flux (Chang et al., 2002; Chang et al., 2006; Klemm et al., 2006; Mildenberger et al., 2009). However, how fog interacts with the LH flux remains unclear from a climatological perspective, in which the long-term observation diurnal analysis is required.

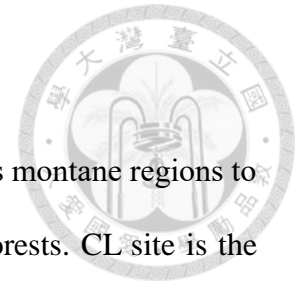
Taiwan, where mountains account for about 60% of the island, is suitable for



studying the hydro-climatology in the montane cloud-fog forest, mainly located at 1500m to 2500m above mean sea level (Schulz et al., 2017; Thies et al., 2015). Long-term flux tower observations were implemented in different types of forests (Chen & Li, 2012; Chu et al., 2014; Klemm et al., 2006; Maneke-Fiegenbaum et al., 2018; Wey et al., 2011). The hydro-climatological characteristics in precipitation and LH flux can reflect the differences between Taiwan's montane cloud-fog forest and non-cloud-fog forest. Higher annual precipitation but lower LH flux in Chi-Lan (CL) montane cloud-fog forest compared to LienHuaChih (LHC) non-cloud-fog forest can be seen. More importantly, an asymmetric diurnal cycle of LH flux with an early peak at 9 a.m. was found in CL montane cloud-fog forest (Fig. 1.1). This diurnal structure of LH flux is not in the same phase with net radiation, but with a couple of hours earlier than the net radiation. In contrast, such a phenomenon cannot be observed in LHC non-cloud-fog forest.

Our study aims to investigate relations between LH flux and fog in montane cloud-fog forest from diurnal and climatological perspectives. The present study will focus on how the asymmetric LH flux affects near-surface meteorology in montane cloud-fog forests, why the asymmetric LH flux occurs and whether the land or atmospheric forcing controls the emergence of the asymmetric LH flux. We hypothesize that the early peak of LH flux may cool down the temperature in the morning of the montane cloud-fog forest, and canopy water may be a key factor to the early peak of LH flux. The analyses compared the meteorological data from flux tower observations between CL montane cloud-fog forest and LHC non-cloud-fog forest. Besides, we conducted several offline land model simulations to examine the contribution of canopy water to the peak of LH flux in CL montane cloud-fog forest. Sensitivity tests were analyzed to find the controlling factors of the asymmetry of LH flux.

Chapter 2 Data and Methodology

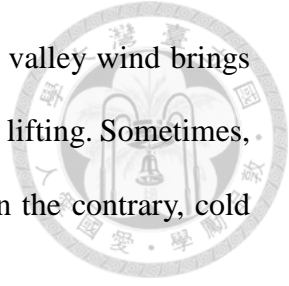


We compared the datasets from two flux tower sites in Taiwan's montane regions to display the hydro-climatological cycle's uniqueness in cloud-fog forests. CL site is the cloud-fog forests with little human interference in Taiwan, featuring frequent afternoon fog. LHC site, where fog seldom occurs, is a reference site as the non-cloud-fog forests. Besides, offline modelling experiments were designed to distinguish the critical physical processes in LH fluxes and to determine the controlling factors to the asymmetry of LH flux in CL.

2.1 Site Description

Located in northeastern Taiwan, the CL flux tower site ($24^{\circ}35'N$, $121^{\circ}25'E$) is at 1650m above mean sea level height (Fig 2.1). CL is characterized by coniferous forests, which is dominated by Taiwan yellow cypress (*Chamaecyparis obtuse var. formosana*) ranging from 11 to 13m height and the understory is carpeted with a large number of epiphytic bryophytes (Chang et al., 2002; Chu et al., 2014) (Fig 2.3). Based on the observation from 2015 to 2017, the leaf area index (LAI) ranges from 3.3 to $5.7m^2/m^2$. The flux tower, with 25m height, was built on a 14° mountain slope toward the southeast side. Fog is detected by the visibility sensor. Following the World Meteorological Organization's definition, we determined the visibility being less than 1km as fog signals. From 2008 to 2011, the time when CL is immersed in foggy conditions accounts for 1/3 of time in this period. The frequency of fog occurrence is higher than 50% from 3 p.m. to 6 p.m. This frequent afternoon fog is observed in all seasons, while the duration of fog tends to be longer in winter due to the coverage of stratus cloud caused by the northeasterly monsoon. The meteorological record shows the annual mean temperature is around $15^{\circ}C$ and annual precipitation is around 3915mm. However, the precipitation type

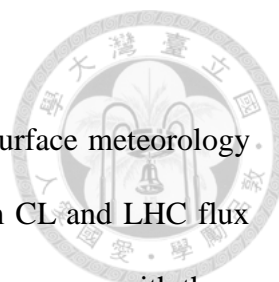
varies from seasons. In summer, local circulation dominates and the valley wind brings warm and humid air. The precipitation usually results from orographic lifting. Sometimes, Taiwan may suffer from heavy rain due to typhoon and Mei-Yu. On the contrary, cold frontal lifting provides the source of precipitation in winter.



Surface fluxes in CL were collected through the eddy covariance method. According to Chen (2016), LH flux, sensible heat flux (SH) and ground heat flux (G) occupied 49%, 35%, and 0.6% of the net energy in the ecosystem, respectively. Net radiation (Rn) is obtained by radiometer at the top of the flux tower, and the storage term (S) can be acquired by the temperature profile in the forest. The annual averaged energy balance closure is 0.86. Under foggy condition, the energy balance closure is merely about 0.6, indicating an imbalanced energy budget.

$$\text{energy balance closure} = \frac{LH + SH}{Rn - G - S}$$

LHC site (23° 55' 52''N, 120° 53' 59''E) is located in central Taiwan with an elevation of about 780m above mean sea level (Fig 2.2). As an example of non-cloud-fog forest in Taiwan, LHC site is dominated by mixed evergreen broadleaved forests whose canopy height is about 17m. During growing seasons, the leaf area index ranges from 2.5 to 4.5m²/m². The flux tower was built on the top of a hill ridge in sub-watershed No.5 at LHC Research Center (Chen & Li, 2012). According to the meteorological observations from 2009 to 2013, the climate in LHC is warm and wet, but less wet than CL. The annual temperature is around 19°C and the annual precipitation is about 2264mm with apparent seasonality. Sometimes LHC would suffer from drought during winter because it is at the lee side of the prevailing winter monsoon. The energy balance closure in dry seasons is about 1, while that in wet seasons is about 0.8 (Chen & Li, 2012).



2.2 Observational Datasets

To understand the effects of the asymmetric LH flux on near-surface meteorology and hydro-climatology, we compare the observational datasets from CL and LHC flux tower sites. The observations from 2008 to 2011 in CL were used to compare with those from 2009 to 2013 in LHC. The observational period mismatched because CL flux tower collapsed during the typhoon season in 2012.

2.2.1 Near-surface meteorological variables

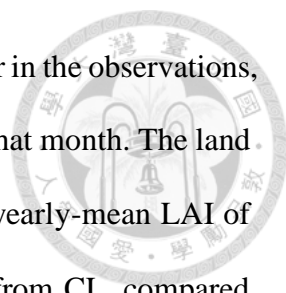
Half-hourly meteorological data, including temperature, humidity, wind field, precipitation, and radiation, were analyzed. We selected no-rain days to explore the reduction of surface fluxes by the fog only. The visibility data were used to distinguish the fogless and foggy conditions at each time step.

2.2.2 Leaf Wetness Measurements

In CL, four leaf wetness sensors were set up at 5.3m, 8.3m, 11.2m, and 14.2m height, respectively, and we analyze the lower three sensors since they performed more stable and continuously. A sensor threshold of 250mV represents dry canopy, while the higher value represents the wetter canopy. The difference between 6 a.m. and 9 a.m. were calculated to show the evolution of canopy wetness in the early morning. Note that 6 a.m. is the time when the sun rises, and 9 a.m. is the time when LH flux reaches the peak.

2.3 Model simulations

We applied the Community Land Model (CLM, version 4) in the Community Earth System Model (CESM, version 1.0.3) to decompose the LH flux using the half-hourly observations from 2008 to 2011 as the atmospheric forcing, including temperature, pressure, specific humidity, wind speed, precipitation, downward solar radiation and downward longwave radiation. The repeating 4-year forcing was run for a total of 24



years, while the last 8 years were analyzed. When we got not a number in the observations, we fill in the corresponding value in climatological diurnal cycle of that month. The land type was set as a 100% needleleaf evergreen temperate tree with a yearly-mean LAI of around $4.6m^2/m^2$. We took 6 branches of Taiwan yellow cypress from CL, compared their weight between dry and totally wet conditions to obtain the coefficient of the maximum allowed dew of 0.2533mm in $1m^2/m^2$ of LAI, while the default value is 0.1mm. Fog's signal was included in the downward solar radiation forcing. However, the canopy did not capture this additional fog water because the precipitation observation was hard to capture the horizontal fog deposition. To make the simulation more realistic, we add additional precipitation forcing by 0.2mm per 30mins according to Chang et al. (2006), when the fog occurrences (observational visibility is less than 1km).

Two offline simulations, with and without canopy water scenarios (hereafter CTR and EXP, respectively), were conducted to show the contribution of canopy water on the LH flux (Table 2.1). In CTR, the canopy water may come from fog deposition, precipitation, and dew. However, the canopy was not allowed to hold any water in EXP. The water would drip into the soil directly right after it formed or be intercepted on the canopy.

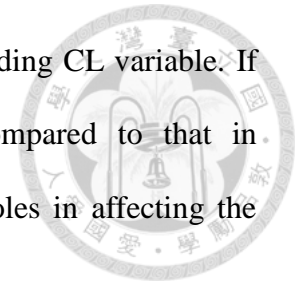
To explore the contribution of different sources of canopy water on the asymmetric LH flux in CL, we further conducted two simulations: Rain+Dew and DEWonly (Table 2.2). In CL, canopy water contains fog, rain and dew, all of which are considered as sources of canopy water in CTR. Rain+Dew excluded fog from the precipitation forcing in CTR. DEWonly, in which coefficient of interception was converted to zero, lose the ability to intercept, prohibiting all canopy water but dew on the canopy. From these three simulations, we can quantify the contribution of different sources of canopy water on LH flux. The difference of LH flux between CTR and Rain+Dew shows the contribution of

fog water, and that between Rain+Dew and DEWonly indicates the contribution of precipitation, and the LH flux in DEWonly reflects the contribution of dew.

To investigate the controlling factors to the asymmetric LH flux in CL, two groups of modelling experiments were conducted. First, whether the asymmetric LH flux results from the setting of the land surface or the atmospheric forcing in the model should be tested. Since we cannot find the asymmetric LH flux in LHC, we respectively utilized the characteristics of land or atmosphere in LHC to distinguish the effect of the land surface setting and the atmospheric forcing on the asymmetry of LH flux. The first group of modelling experiment consists of CTR_3yr, LHCatm_CLsurf, and CLatm_LHCsurf (Table 2.3). To ensure that the atmospheric forcing was not influenced by different inter-annual variability, we selected the overlapping year in both CL and LHC observational data, from 2009 to 2011, as the simulated year. The repeating 3-year atmospheric forcing was run for 24 years, while the results of the last 8 years were analyzed. CTR_3yr use CL's atmospheric forcing from 2009 to 2011, and the setting of the land surface is still the same as CTR. In LHCatm_CLsurf, the setting of land surface remains the same as CTR, but the atmospheric forcing was replaced by LHC atmospheric forcing. On the contrary, the CL atmospheric forcing remains in CLatm_LHCsurf, but the setting of land surface was changed to LHC. The LHC land surface in the model is composed of 42.2% needleleaf evergreen tree, 38.6% broadleaf evergreen tree, 19.2% broadleaf evergreen shrub. Yearly mean LAI is set to be $3.95m^2/m^2$, based on 11-year observation from 2008 to 2018. The coefficient of the maximum allowed dew was set as default, 0.1mm in $1m^2/m^2$ of LAI.

The second group of modelling experiments were conducted to understand which variables in the atmospheric forcing has greater contribution to the asymmetric LH flux (Table 2.4). We set the land surface as CTR, used LHC atmospheric forcing and

respectively replaced each variable in the forcing by the corresponding CL variable. If this sensitivity test can find a more asymmetric LH flux compared to that in LHCatm_CLsurf, those atmospheric variables may play critical roles in affecting the hydro-climatological cycle in montane cloud-fog forests.



Chapter 3 Results



3.1 The impact of the asymmetric LH flux on the formation of the afternoon fog

The asymmetric LH flux in CL montane cloud-fog forest can induce slow-increased near-surface air temperature and provide early water vapor source to the boundary layer. First, the air temperature increased slowly in the morning because most of the energy is used for evapotranspiration. The tendency of the net radiation and LH is quite consistent from 6 to 9 a.m. (Fig. 1.1). Thus, less energy was used to heat the near-surface atmosphere, making diurnal temperature range smaller, with only 2 °C, in CL montane cloud forest. In contrast, the net energy gained over the LHC forest region was not mainly used for evapotranspiration; therefore, the diurnal temperature range was 3 times larger than CL (Fig. 3.1a). Second, the early peak of LH flux at 9 a.m. can provide local water vapor to the atmosphere. In addition to the local water vapor contribution, enhancing valley wind prevailing from dawn to the afternoon may bring water vapor from lowland forests to flux tower sites (Fig. 3.1b; Fig. 3.1c). Although we cannot distinguish either advection or local contribution from total water vapor supply between two sites, it is observed that specific humidity keeps increasing from 6 a.m. to 3 p.m. in both places (Fig. 3.1b).

Because of the small diurnal temperature range in CL, water vapor can easily reach saturated at about 3 p.m., whereas in LHC, the near-surface air temperature is too high to make water vapor saturate in the afternoon. As a function of temperature and water vapor, relative humidity keeps increasing from 7 a.m. to 5 p.m. in CL. Almost 100% of mean relative humidity and its small variation during the afternoon indicate the signal of frequent fog (Fig. 3.1d).

3.2 The importance of canopy water to the asymmetric LH flux

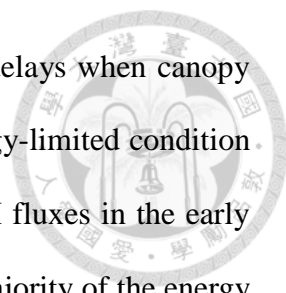
The fog water may be intercepted by the canopy and become a source of canopy water. Because relative humidity remains high during the nighttime in CL, the intercepted fog water can usually sustain until the next morning. Leaf wetness sensors indicated a significantly wetter canopy at 6 a.m. compared to that at 9 a.m. (Table 3.1). This drying trend from 6 to 9 a.m. displayed that canopy water may have a strong contribution to the peak of LH flux in CL.

CTR and EXP simulations were conducted to demonstrate the contribution of canopy water to the asymmetric LH flux. In the CTR simulation, canopy water keeps accumulating in the afternoon and reaches its peak at about 6 a.m. (Fig. 3.2a). It can capture the asymmetry of LH flux despite a one-hour delay of the peak of LH flux compared to the observation. On the contrary, the EXP simulated a symmetric LH flux with the peak at about 11 a.m., which is in the same phase as net radiation (Fig. 3.2b). After decomposing LH flux, we found that the early peak of LH flux in CTR is dominated by the canopy evaporation, while the peak of LH flux in EXP is dominated by the transpiration. In CTR, 71% of LH flux is from the canopy evaporation, and the peak of canopy evaporation is in phase with the drying trend of canopy water in the early morning. A sharp increase in canopy evaporation before 10 a.m. results in more than 50% decrease in the canopy water within 3 hours after the sun rises. The transpiration in CTR is in phase with net radiation because of the photosynthesis processes. However, the peak value of transpiration is merely half of the canopy evaporation. Thus, the early peak of LH flux can be attributed to the high canopy evaporation at around 9 a.m. (Fig. 3.2c). Without the canopy water but with the same net radiation acquisition, EXP simulates a symmetric LH flux of which transpiration accounts for 83% (Fig. 3.2d).

3.3 Canopy water sensitivity test

The canopy water source can be composed of fog, precipitation, and dew, which accounts for 31%, 61%, and 8% of total canopy water, respectively (Fig. 3.3a). The contribution of fog and precipitation on canopy water keeps increasing in the afternoon, and such a large amount of water persists throughout the night. Dew starts to form at night and also keeps increasing until the dawn. The canopy water reaches their peak at dawn and soon decreases after sunrise, thus contributing to high canopy evaporation in the early morning.

In the comparison among experiments of CTR, Rain+Dew, and DEWonly, we found that the more the canopy water at dawn is, the higher the peak of LH flux is (Fig. 3.3a; Fig 3.3b). Although DEWonly contains the least canopy water among the three experiments, it can simulate an asymmetric diurnal LH flux. Comparing DEWonly with Rain+Dew, we obtained an increase in LH flux during the daytime by precipitation, with 135.6 mm/year, whereas fog causes an increase with 100.9 mm/year in LH flux, comparing CTR with Rain+Dew. These increases in LH flux are mainly derived from the increases in canopy evaporation in the early morning. However, canopy evaporation competes with transpiration in terms of their contribution to LH flux (Fig. 3.3c). This competing effect might be attributed to canopy resistance regulated by canopy water. When stomata is covered by water, water vapor tends to be more easily to exchange to the atmosphere through evaporation rather than transpiration. From DEWonly to CTR, the peak of canopy evaporation becomes larger, but that of transpiration becomes smaller. Comparing Rain+Dew with DEWonly, the increase in canopy evaporation is 190.6 mm/year, and the decrease in transpiration is 53 mm/year. Comparing CTR with Rain+Dew, the increase in canopy evaporation is 138.1 mm/year, and the decline in transpiration is 36.3 mm/year.

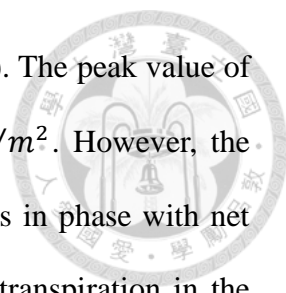


It is noted that the timing of the peak of canopy evaporation delays when canopy contains more water (Fig. 3.3c). The delay is derived from the energy-limited condition in the early morning. Net radiation pretty matches the values of LH fluxes in the early morning before the LH fluxes reach their peaks, which means the majority of the energy that the forest gains is used for evapotranspiration. This situation can also be seen in the observation (Fig. 1.1). LH flux is affected by available water and available energy. In CL, plentiful canopy water serves as the major available water in the early morning, and net radiation is largely allocated to LH flux at the same time. Under energy-limited condition, if the canopy contains more water in the early morning, it will take longer to evaporate the extra canopy water, and canopy evaporation is able to keep rising compared with less canopy water scenarios.

3.4 The controlling factors to plentiful canopy water before sunrise

3.4.1 The land surface type or the atmospheric forcing?

In offline model simulations, both the setting of land and the atmospheric forcing may influence the simulation results. The comparison between CTR_3yr and CLatm_LHCsurf will show the impacts of different land surface types on LH flux, while the comparison between CTR_3yr and LHCatm_CLsurf will show the impacts from the atmospheric forcing. In CLatm_LHCsurf, we still can find the asymmetric LH flux although the peak is lower than that in CTR_3yr by 56.7 W/m^2 (Fig. 3.4a). Such a decrease in total LH flux caused by the change of land type from CL to LHC is approximately 0.2 mm/day. The asymmetric LH flux is also attributed to high canopy evaporation in the early morning, similar to the mechanism in CTR_3yr. Despite a decrease in the average of canopy water by 0.4 mm, the total canopy evaporation still

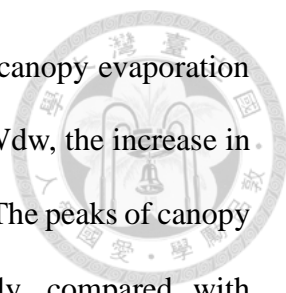


outweighs the total transpiration by 0.1 mm/day (Fig. 3.4b; Fig 3.4c). The peak value of canopy evaporation is larger than that of transpiration by $12.1 W/m^2$. However, the diurnal cycle of LH flux in LHCatm_CLsurf is symmetric, which is in phase with net radiation. This symmetric LH flux results from the dominance of transpiration in the partition of LH flux. The peak value of transpiration outweighs that of canopy evaporation, and the diurnal cycle of transpiration is in phase with net radiation because of photosynthesis process. Therefore, it is the atmospheric forcing that contributes more to the asymmetry of LH flux.

3.4.2 Sensitivity test of the atmospheric forcing

In CTR_3yr, the diurnal pattern of LH flux is asymmetric, and the LH amount is composed of canopy evaporation (68.2%), transpiration (31.1%), and ground evaporation (1%) (Figure 3.5). Canopy evaporation is the majority of total LH flux. However, after we changed the atmospheric forcing to LHC, the diurnal cycle of LH flux became symmetric. The proportion of canopy evaporation, transpiration and, ground evaporation are 23.3%, 75.1%, and 1.1%, respectively, in the total LH. From LHCatm_CLsurf to CTR_3yr, LH flux gets asymmetric with the increase in the proportion of canopy evaporation and the decrease in transpiration. Analysis from the sensitivity tests shows that wind speed, precipitation, temperature, downward solar radiation, and downward longwave radiation all have positive impacts on the increase in canopy evaporation, compared with LHCatm_CLsurf. Among all the variables, precipitation, temperature, and downward longwave radiation are the top three contributors to the increase in the proportion of canopy evaporation, which is by 29.3%, 10%, and 6.6%, respectively, compared with LHCatm_CLsurf.

Two possible reasons may cause an increase in the proportion of canopy evaporation: the increase in the absolute value of canopy evaporation or the decrease in other partition



components of LH fluxes. Figure 3.6a displays the diurnal cycle of canopy evaporation in each sensitivity test. In LHCatm_CL_precip and LHCatm_CL_LWdw, the increase in the proportion of canopy evaporation results from the former reason. The peaks of canopy evaporation increase by $75.6 W/m^2$ and $28 W/m^2$ respectively, compared with LHCatm_CLsurf. The corresponding increase in total canopy evaporation in the two simulations are by 0.8 and 0.02 mm/day, respectively. After we change the precipitation forcing from LHC to CL, the average of canopy water increases 0.3 mm (Fig 3.6b). Canopy accommodates 0.42 mm more water than LHCatm_CLsurf at dawn, resulting in a higher peak value of canopy evaporation in the early morning. LHCatm_CL_LWdw shows the increase in the average of canopy water by 0.05 mm and such increase majorly happens at night, probably because of dew formation. The longwave radiation in CL is lower, by an average of $24.4 W/m^2$, than LHC at night. Besides, the increase of the proportion of canopy evaporation in LHCatm_CL_T may be attributed to the decrease in other partition components of LH fluxes. The canopy evaporation does not show much difference with LHCatm_CLsurf; however, the transpiration decreases by 205.1 mm/year when we change the temperature forcing to CL. This reduction might result from a relatively low temperature in CL. The difference of mean diurnal temperature between CL and LHC is $4.4^\circ C$. In summary, through the sensitivity tests, the precipitation forcing may be the main controlling factor to plentiful canopy water in the early morning.

Chapter 4 Discussion



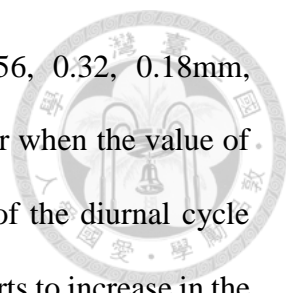
4.1 The signal of the asymmetric LH flux

Some may concern whether the asymmetric LH flux in CL is a signal of climatological average with daily maximum happens in different timing in the morning, or the peak of LH flux does frequently happen at 9 a.m. Figure 4.1 shows the occurrence probability of daily maximum LH flux in CL and LHC. The high occurrence probability of daily maximum LH flux in the two places both happens at the timing of the climatological peak of LH flux. The highest occurrence probability of daily maximum LH flux in CL is at 8:30 a.m., and the maximum of the diurnal cycle of LH flux happens at 9:30 a.m. In LHC, the highest occurrence probability of daily maximum LH flux is at 11:30 a.m., and the maximum of the diurnal cycle of LH flux happens at noon. To sum up, the asymmetric diurnal cycle of LH flux does result from the frequent peak timing around 9 a.m.

4.2 The sensitivity test of maximum allowed canopy water

To show the modelling impact of maximum allowed canopy water on the asymmetry of LH flux in CL, the sensitivity test according to the coefficient of maximum allowed dew were conducted: CTR, max_cw_0.2, max_cw_0.1, max_cw_0.05. The coefficient of maximum allowed dew regulates maximum allowed canopy water by multiplying the coefficient with LAI in the model. In these four simulations, the atmospheric forcing and the land type are fixed as CTR, but the coefficient of the maximum allowed dew were conducted to 0.2533, 0.2, 0.1, 0.05 mm in $1m^2/m^2$ of LAI, respectively.

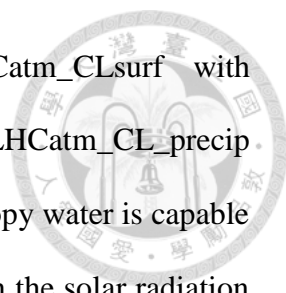
Figure 4.2 displays the comparison of the diurnal cycle of canopy water, LH flux and the partition of LH flux among CTR, max_cw_0.2, max_cw_0.1, max_cw_0.05. The



daily mean canopy water in the four simulations are 0.68, 0.56, 0.32, 0.18mm, respectively. Although the daily mean canopy water becomes smaller when the value of the coefficient of maximum allowed dew gets smaller, the pattern of the diurnal cycle does not change significantly. The canopy water in all simulations starts to increase in the afternoon, reach the peak at dawn and soon decrease before 9 a.m. (Fig. 4.2a) Compared max_cw_0.05 with CTR, the total LH flux decreases by 23%. The ratio of the decrement in total LH flux in max_cw_0.1 and max_cw_0.2 are 15% and 4%, respectively (Fig. 4.2b). The decrements in the total LH flux are mainly derived from the decreases in canopy evaporation. In max_cw_0.05, the peak value of canopy evaporation is less than that in CTR by 28.6% because of less canopy water at dawn. The decrement ratio of canopy evaporation in max_cw_0.1 and max_cw_0.2 are 13.5% and 3.6%, respectively compared with CTR (Fig. 4.2c). Although less canopy water at dawn cause less canopy evaporation in the morning, the peak value of canopy evaporation still outweighs the peak value of transpiration. Therefore, the asymmetric LH flux with peaks at about 9 or 10 a.m. can be found in the four simulations.

4.3 The drizzle's effect on the asymmetry of LH flux

In the comparison of the observed precipitation between CL and LHC, CL rains more frequently and the drizzle in CL (the precipitation is less than 5mm) is more likely to happen than that in LHC. Figure 4.3 indicates the comparison of probability density function in precipitation between CL and LHC. The zero category shows the probability of no-rain data, which is 0.85 in CL and 0.92 in LHC. Aside from 0 mm, the probability of precipitation less than 5 mm, with 0.5 as an interval of the category, is larger in CL than in LHC. From the sensitivity tests of the atmospheric forcing, precipitation was found to be the controlling factor to the asymmetric LH flux. The storage of canopy water

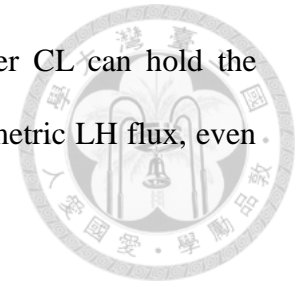


increases the most in LHCatm_CL_precip. Compared LHCatm_CLsurf with LHCatm_CL_precip, more frequent drizzle input on the canopy in LHCatm_CL_precip results in the larger storage of the averaged canopy water. More canopy water is capable of evaporating in the early morning in LHCatm_CL_precip although the solar radiation forcing remains the same as LHCatm_CLsurf. Therefore, the frequent drizzle phenomenon in CL may be highly associated with the increase in the diurnal cycle of canopy water.

To investigate the effect of frequent drizzle on the asymmetry of LH flux, we conducted a more idealized simulation. We calculated the climatological diurnal cycle of precipitation from 2009 to 2011 LHC atmospheric forcing. This climatological diurnal cycle differed every month but repeated every day in each month. We replaced the original precipitation forcing by this climatological diurnal cycle, and let the rest of the atmospheric forcing remained the same as observations. We also use the same land surface as CL (Table 4.2) in this experiment. In this simulation named LHCatm_Clim_precip, drizzle always happens and the probability of precipitation under 1 mm is much higher than LHCatm_CLsurf (Fig 4.4a). With the drizzle's effect, the averaged canopy water becomes approximately twice more than that in LHCatm_CLsurf (Fig 4.4b). The accumulating rate is higher, especially at night, making the peak value of canopy water become twice higher, compared to LHCatm_CLsurf. Despite the twice higher peak of the canopy water, the peak of canopy evaporation reaches 3 times larger in the early morning. Also, 29% of total transpiration is reduced (Fig 4.4c). Thus, the diurnal cycle of LH flux becomes more asymmetric with an early peak at about 10 a.m. (Fig 4.4d)

Based on the two simulations, if the frequency of drizzle is significantly reduced, we will lose the characteristics of the asymmetric LH flux because of the disappearance of

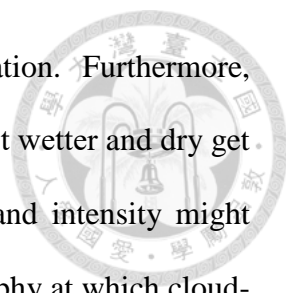
high canopy evaporation in the early morning. Therefore, whether CL can hold the characteristics of the frequent drizzle may be essential to the asymmetric LH flux, even the effect on fog formation.



4.4 The diurnal LH flux and the fog under climate change: a risk or a benefit to the ecosystem in CL?

The small diurnal temperature range, frequent fog, precipitation, and plentiful canopy water plays a vital role in the asymmetric LH flux. How these variables affected by climate change and the corresponding response of the characteristics of hydro-climatology in CL worth further discussion. First, the presence of the canopy water may result in the emergence of the asymmetric LH flux. If the canopy water is absent, the diurnal cycle of the LH flux will be in the same phase with net radiation, likewise the pattern of LH flux and net radiation in the non-cloud-fog forest. This situation indicates if the canopy loses the ability to store the water or the water storage on the canopy is insufficient, the canopy evaporation in the early morning will become lower. In CL, although the no-canopy scenario may be impossible to happen since it is a national protected area, the amount of canopy water may probably vary under climate change due to the change in atmospheric water input.

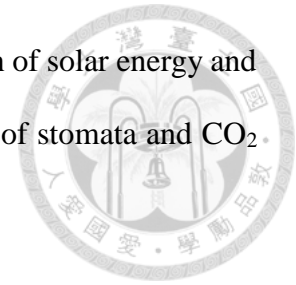
Second, the amount of the canopy water would influence the asymmetry pattern of LH flux. In montane cloud-fog forests, the canopy water in the early morning is derived from fog, dew, and precipitation accumulation since the previous afternoon or night. Recent studies have shown a decrease in fog frequency due to anthropogenic activities. The rising temperature in daytime might cause the water vapor to reach saturation difficultly in the afternoon (Foster, 2001; Still et al., 1999). Besides, the nighttime temperature may influence dew formation. High temperature at night will decrease



relative humidity and have negative impacts on the condensation. Furthermore, precipitation pattern may alter under climate change, such as “wet get wetter and dry get drier” (Dore, 2005). The change in both precipitation frequency and intensity might impact the storage of canopy water (Foster, 2001). Complex topography at which cloud-fog forests are located may shed large uncertainties on the change in precipitation. Both precipitation and fog occurrence might be altered by the change in mountain-valley wind circulation. When the temperature gradient varies between mountain top and valley, the wind magnitude may change. Although the contribution of advection to the water vapor accumulation in CL in the daytime remains unknown, the change in advection might affect water vapor supply, which then change the fog or precipitation climatology, thus influencing the amount of canopy water. If the amount of canopy water is unable to allow canopy evaporation to outweigh transpiration in daytime, the diurnal cycle of LH flux may become symmetric. Such symmetric LH flux will, in turn, enlarge the diurnal temperature range, possibly unfavorable to the afternoon fog formation.

Last but not least, some have concerns the disappearance of fog may have negative impacts on the growth of plants, but a lack of fog might be a benefit to Taiwan’s montane cloud-fog forests. In some seasonal dry regions, the interception of fog is essential to plant water use, especially to the top of canopy. Research has found that fog could support the growth of trees because of their direct water use through foliar water uptake (Dawson & Goldsmith, 2018; Limm et al., 2012). However, in Taiwan’s montane cloud-fog forests where annual precipitation usually exceeds 3000mm, the water probably is not a limiting factor to the ecosystem. When fog disappears, wet leaves can still exist if the precipitation pattern does not change significantly. The lack of fog seems not to negatively influence the available water for the trees, but can significantly increase the available energy for photosynthesis or tree growth. Mildenerger et al. (2009) indicate fog can block about

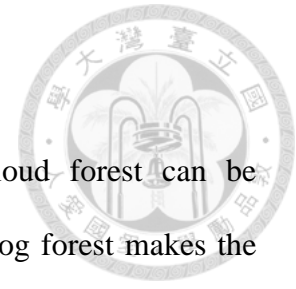
64% of solar radiation. Without the immersion of fog, the acquisition of solar energy and vapor pressure deficit will become larger and might favor the open of stomata and CO₂ uptake.



4.5 The importance of fog description in models

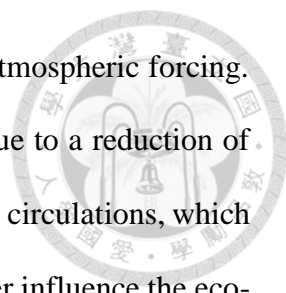
Fog is a source of canopy water that contributes to the asymmetric LH flux. Without fog's effects on the energy and water cycle, the land will receive excess solar radiation, and LH flux will be overestimated. Furthermore, CO₂ uptake in the cloud-fog forest may have bias without fog. Figure 4.5 displays the effect of fog on LH flux and CO₂ flux in the CL montane cloud-fog forest. Approximately 56% of LH flux and 48% of CO₂ flux are reduced under foggy conditions. As a result, if the fog is not considered in models, we may have overestimation on simulating the water exchange between land and atmosphere and the carbon uptake in the montane cloud-fog forests.

Chapter 5 Conclusion



The unique hydro-climatological cycle in CL montane cloud forest can be summarized: (1) the early peak of LH flux in CL montane cloud-fog forest makes the near-surface temperature increase slowly in the morning. (2) During the daytime, valley wind brings water vapor from lowland combined with evapotranspiration from local forest, resulting in water vapor accumulation until 3 p.m. (3) Because of the small diurnal temperature range, water vapor can easily reach saturation in the afternoon, thus favoring fog formation. Fog further serves as a source of canopy water in addition to the dew and precipitation. (4) Plentiful canopy water can sustain throughout the night because of the high relative humidity. The drying trend of leaf wetness after sunrise implies the critical role of canopy water on the early peak of LH flux. This unique hydro-climatological cycle in the montane cloud-fog forest reflects the inseparable relationship between the canopy and near-surface meteorology at the diurnal cycle, and such unique cycle can be seen in all seasons (Fig. 5.1). The offline simulations also suggest the asymmetric LH flux is principally attributed to high canopy evaporation in the early morning.

Fog, precipitation, and dew comprise the plentiful canopy water. From the sensitivity tests, precipitation forcing may be the controlling factor to the plentiful canopy water in the early morning and significantly affect the peak of canopy evaporation. Such abundant canopy water in CL may be attributed to the frequent drizzle phenomenon. Besides, downward longwave radiation and temperature forcing are the minor contributors to the asymmetric LH flux. The downward radiation forcing leads to an increase in nighttime dew, having less contribution compared with precipitation. The change in temperature forcing mainly results in the change in total transpiration, which may affect the asymmetry of LH flux when total transpiration outweighs total canopy evaporation. In



summary, the source of canopy water is highly associated with the atmospheric forcing. Under future projections, a decrease in canopy water may happen due to a reduction of fog formation, a larger variation in precipitation, and a change in local circulations, which could lead to the disappearance of the asymmetric LH flux and further influence the eco-hydroclimatology in the montane cloud forests.

In this study, where the water vapor comes from and how the asymmetric LH flux will be influenced by different atmospheric forcing under climate change remain uncertain. Future works may require isotopic measurement to distinguish local and advection water vapor supply. In addition, idealized model simulation may be needed to discuss how the mean and variance of different atmospheric forcing may respectively affect the hydro-climatological cycle in montane cloud-fog forests.

FIGURES

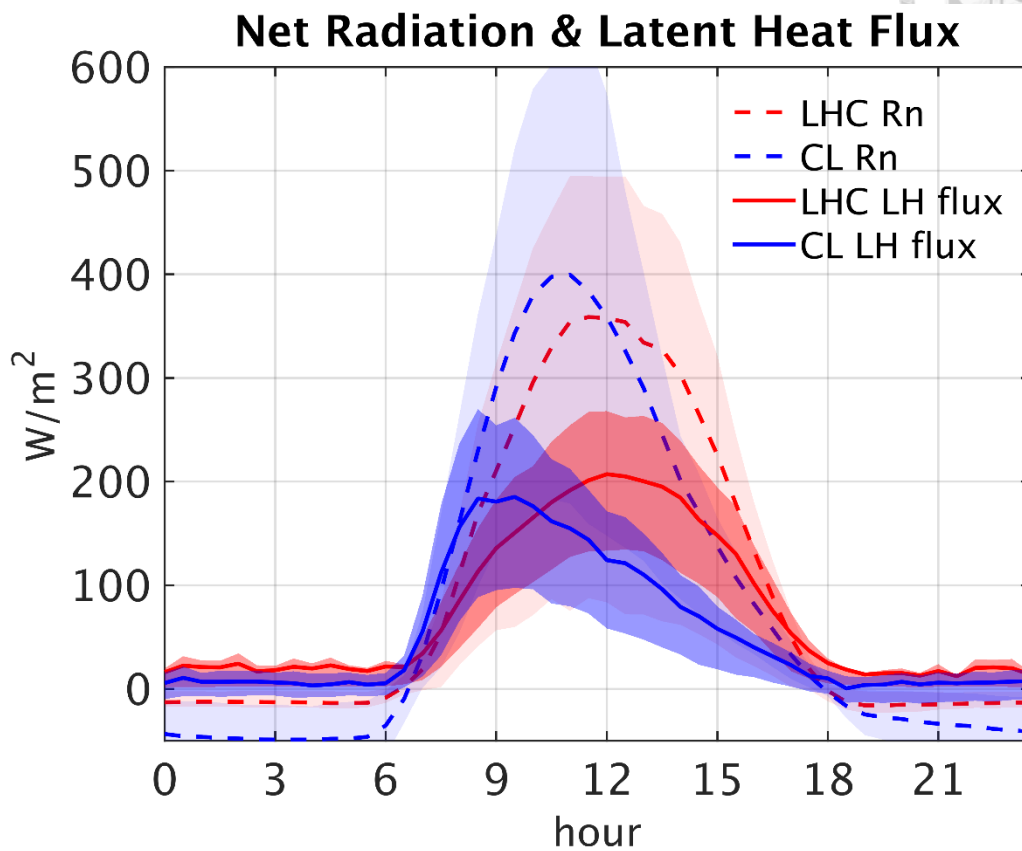


Figure 1.1 The comparison of the diurnal cycle of net radiation (Rn: dashed lines) and latent heat flux (LH flux: solid lines) between CL (Chi-Lan: blue lines) and LHC (LienHuaChih: red lines). The shading color represents the variation of the energy fluxes between the first quartile and the third quartile from four years of data from 2008 to 2011 in CL and two years of data from 2012 to 2013 in LHC.

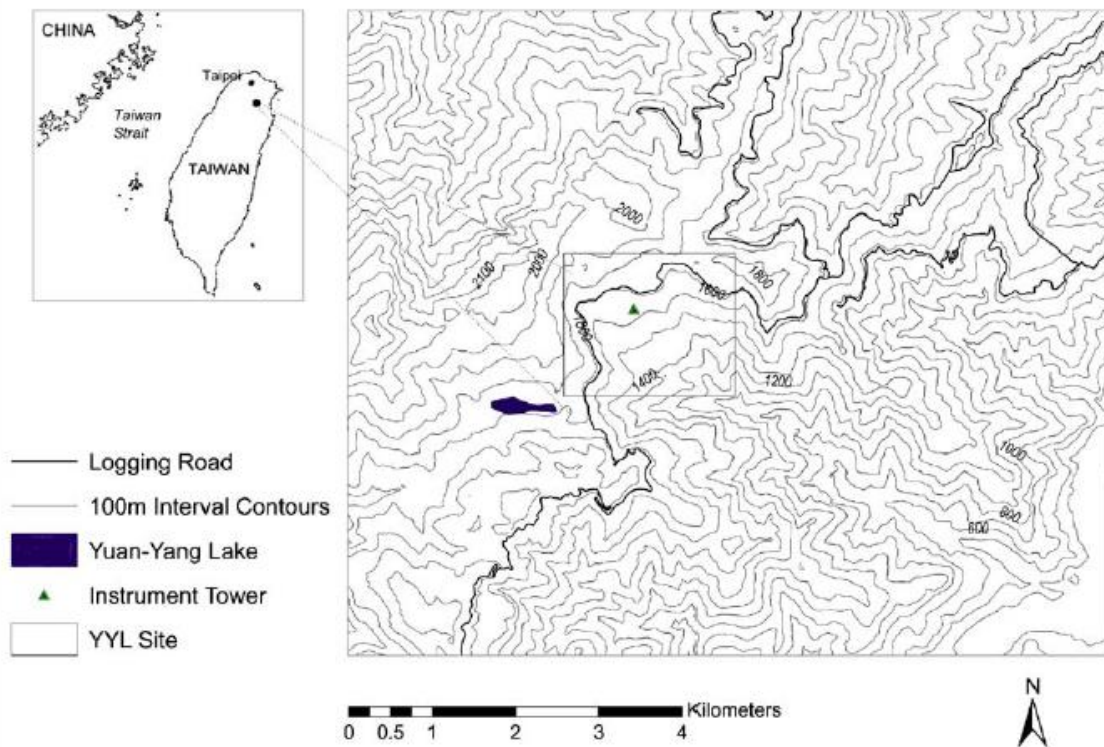


Figure 2.1 The location of CL flux tower site (green triangle). (The figure is taken from Klemm et al. (2006).)

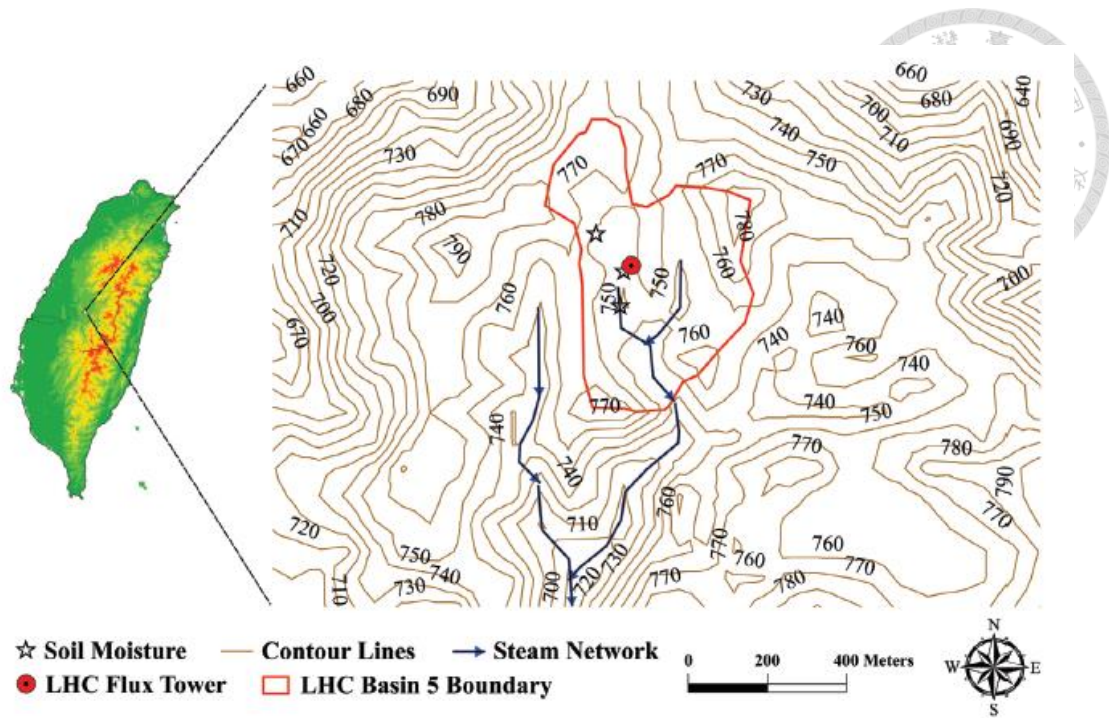


Figure 2.2 The location of LHC flux tower site (red dot). (The figure is taken from Chen et al. (2012).)

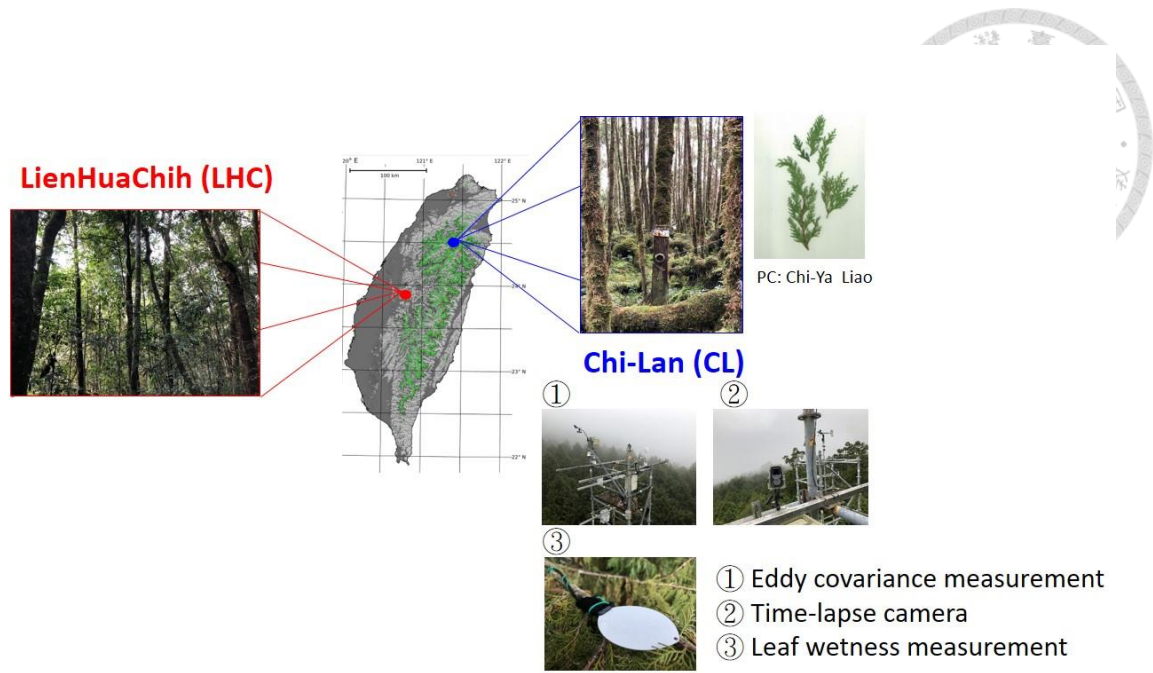


Figure 2.3 The land type comparison between CL and LHC and the measurements in CL. (The middle map in which green area represents the distribution of montane cloud-fog forests in Taiwan is taken from Schulz et al. (2017).)

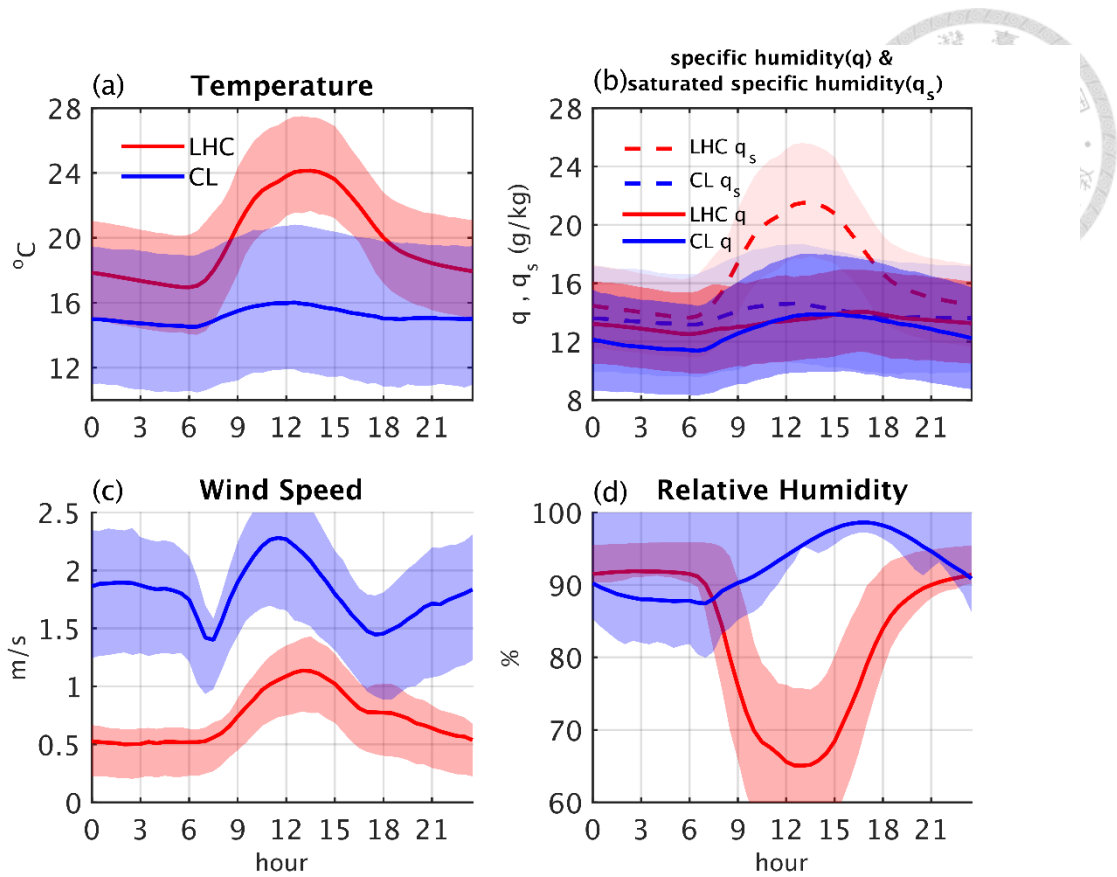


Figure 3.1 Five meteorological variables obtained from the flux towers in CL (blue lines) and LHC (red lines): (a) temperature, (b) specific humidity (solid lines) and saturated specific humidity (dashed lines), (c) wind speed, and (d) relative humidity. The shading color represents the variation of each meteorological variable between the first quartile and the third quartile from four years of data in CL and five years of data in LHC.

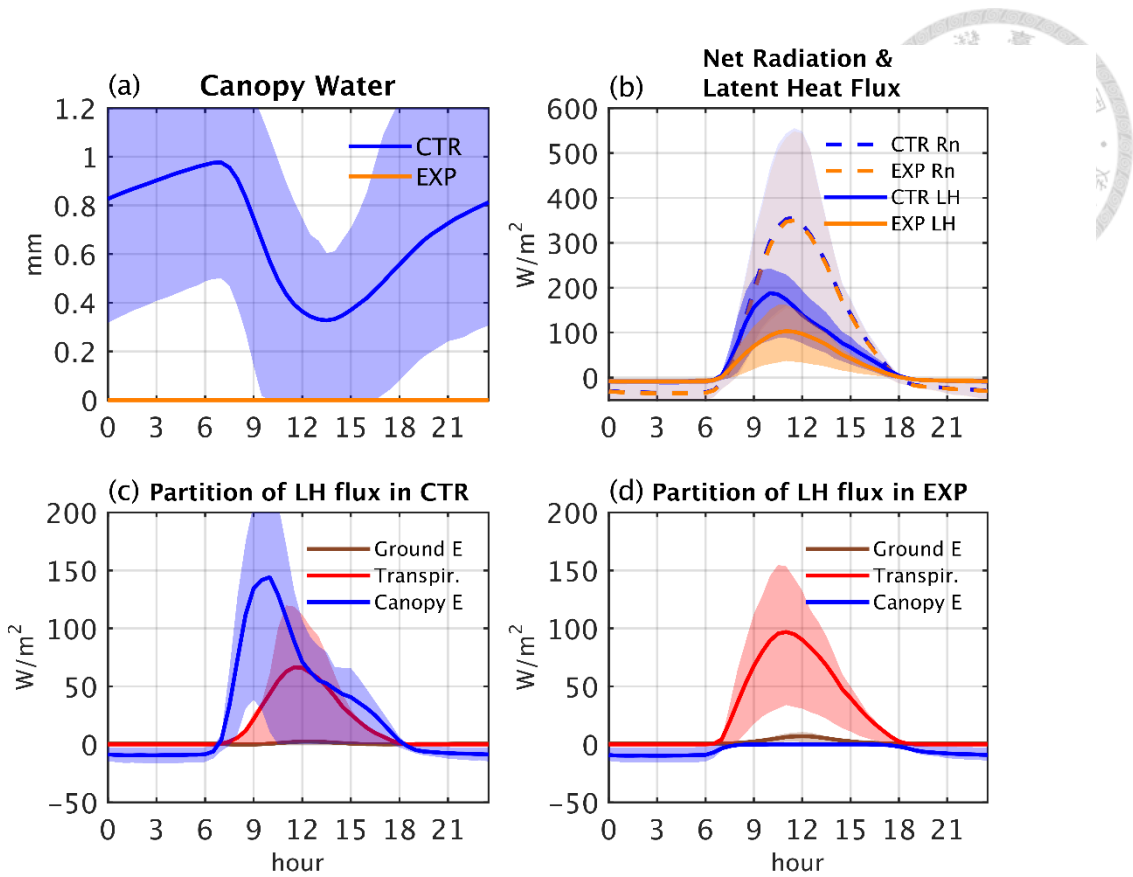


Figure 3.2 (a) Simulations conducted by the Community Land Model V4: with (CTR: blue lines) and without (EXP: orange lines) canopy water representation. (b) The comparison of the diurnal cycle of net radiation (dashed lines) and LH flux (solid lines) between CTR and EXP. (c) (d) The partition of LH flux (including ground evaporation (brown lines), transpiration (red lines), and canopy evaporation (blue lines)) for (c)CTR and (d)EXP. The shading color represents the variation of the energy fluxes between the first quartile and the third quartile from the last eight years of the simulations.

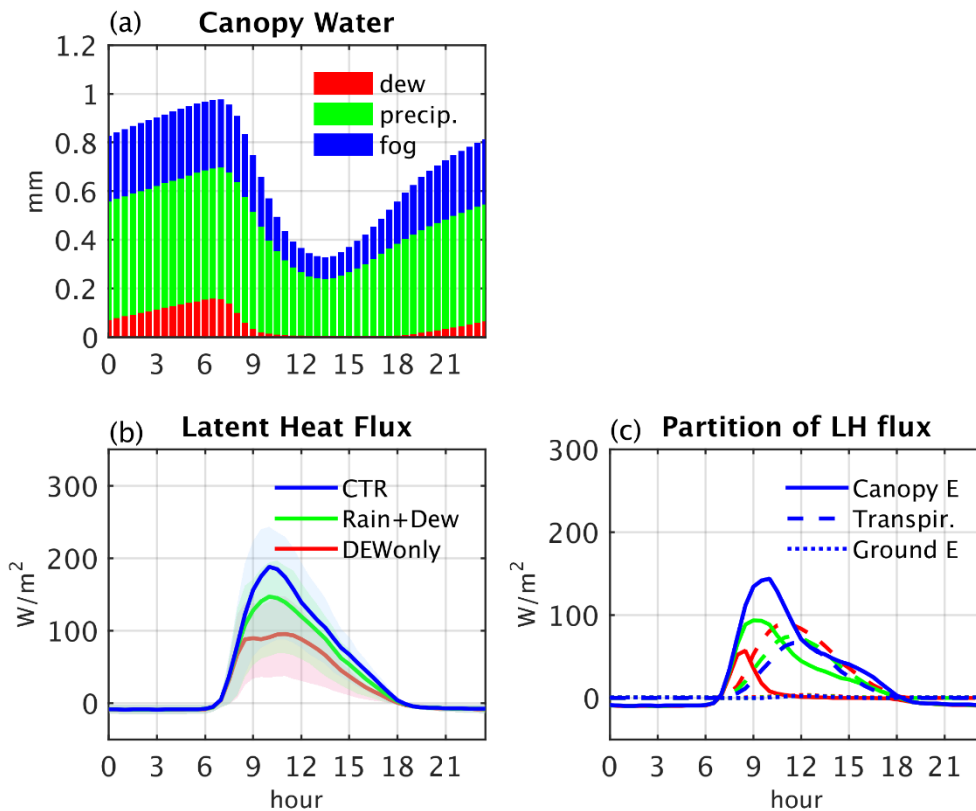


Figure 3.3 (a) The contribution of different source of water on the canopy, including fog (blue bars), rain (green bars) and dew (red bars). (b) The comparison of the diurnal cycle of LH flux among CTR (blue line), Rain+Dew (green line) and DEWonly (red line). The shading color represents the variation of the LH fluxes between the first quartile and the third quartile from the last eight years of each simulation. (c) The partition of LH flux among CTR (blue lines), Rain+Dew (green lines) and DEWonly (red lines). The solid lines, dashed lines and dotted lines represent canopy evaporation, transpiration, and ground evaporation, respectively.

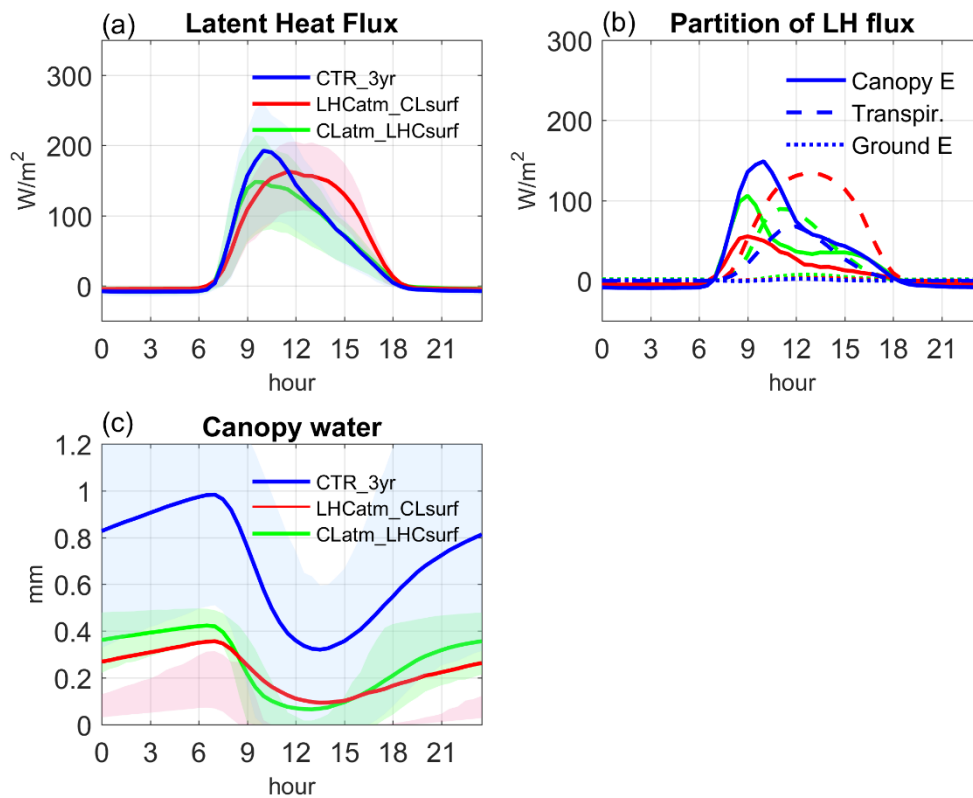


Figure 3.4 (a) The comparison of the diurnal cycle of LH flux among CTR_3yr (blue line), LHCatm_CLsurf (red line) and CLatm_LHCsurf (green line). The shading color represents the variation of the LH fluxes between the first quartile and the third quartile from the last nine years of each simulation. (b) The partition of LH flux among CTR_3yr (blue lines), LHCatm_CLsurf (red lines) and CLatm_LHCsurf (green lines). The solid lines, dashed lines and dotted lines represent canopy evaporation, transpiration, and ground evaporation, respectively. (c) The comparison of the diurnal cycle of canopy water among CTR_3yr, LHCatm_CLsurf and CLatm_LHCsurf. The shading color represents the variation of the canopy water between the first quartile and the third quartile from the last nine years of each simulation.

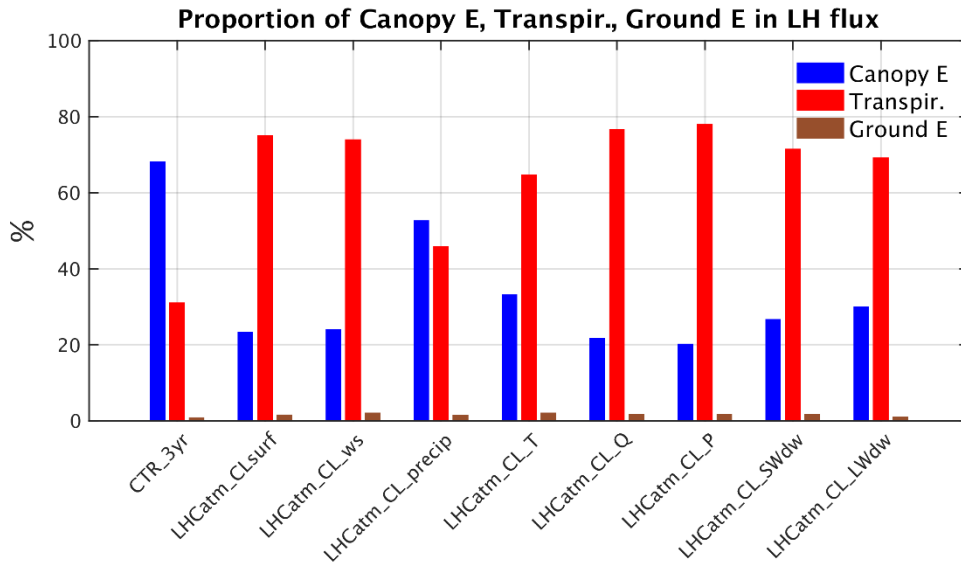


Figure 3.5 Atmospheric forcing sensitivity test: comparing the proportion of the partition of LH flux including canopy evaporation (blue bars), transpiration (red bars) and ground evaporation (brown bars).

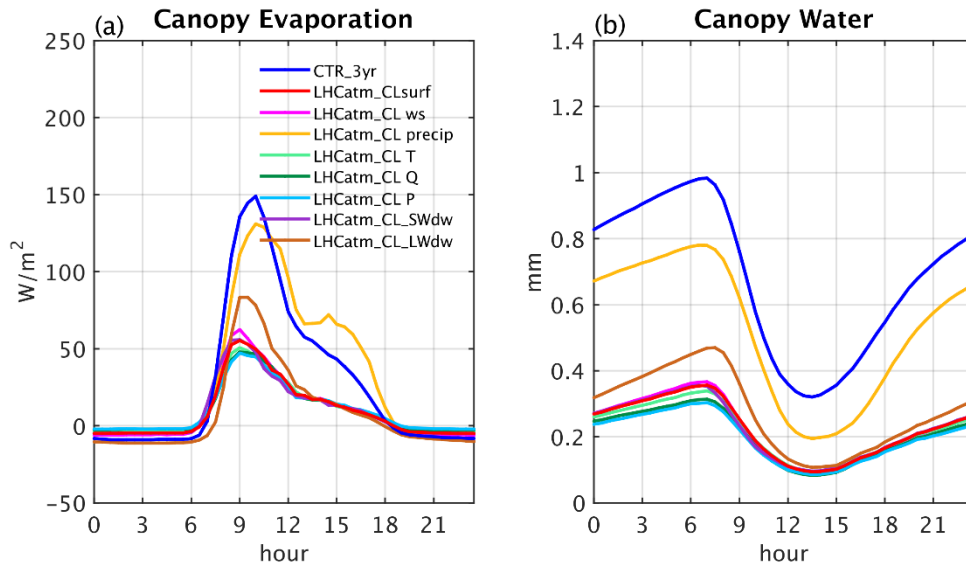


Figure 3.6 Atmospheric forcing sensitivity test: comparing (a) canopy evaporation and (b) canopy water in each sensitivity run with CTR_3yr and LHCatm_CLsurf.

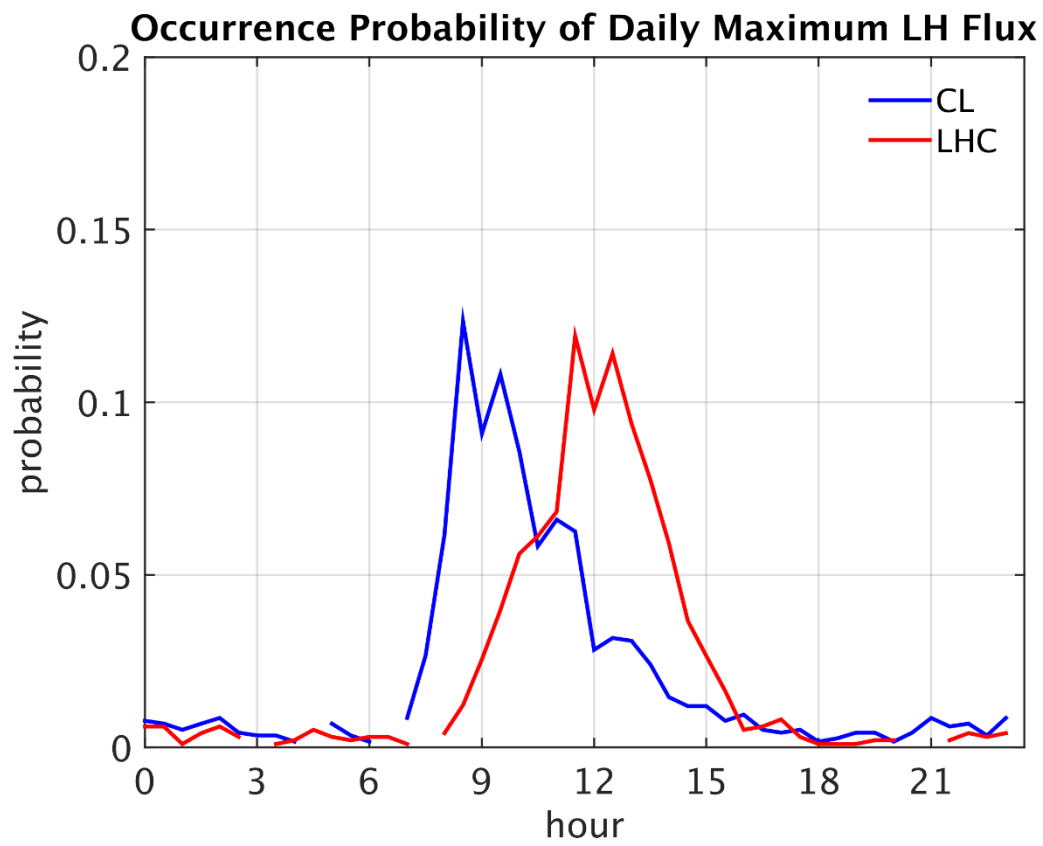


Figure 4.1 The comparison of the occurrence probability of the daily maximum LH flux between CL (blue line) and LHC (red line).

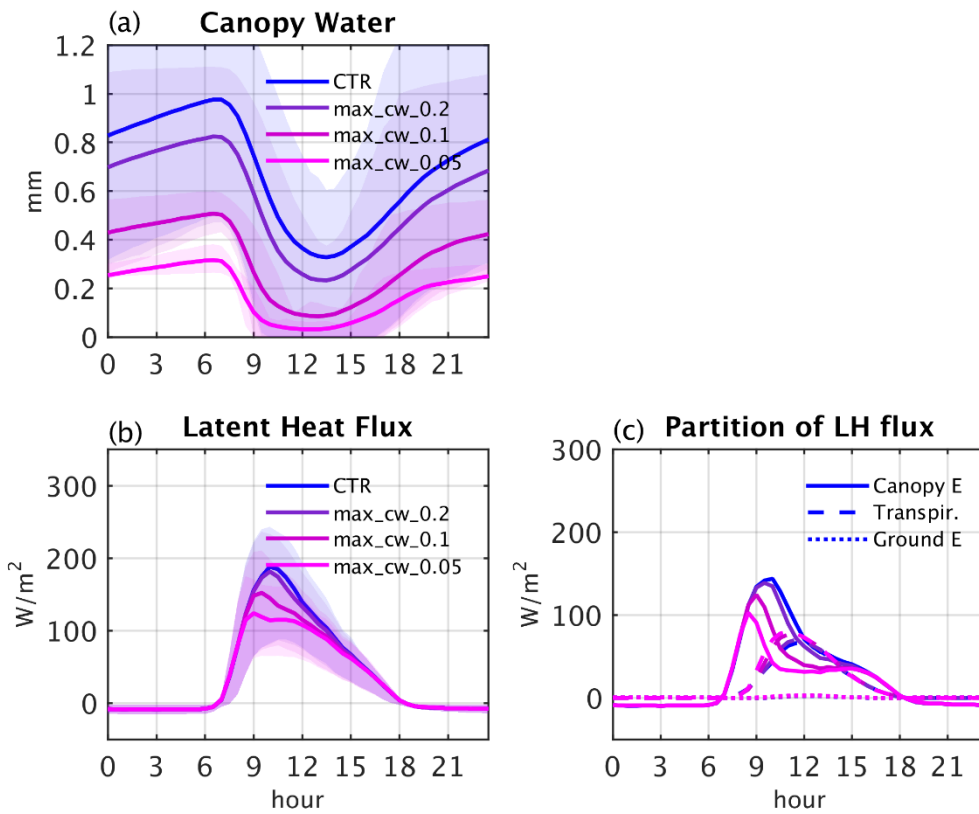


Figure 4.2 (a) The comparison of the diurnal cycle of canopy water among CTR (blue line), max_cw_0.2 (purple line) and max_cw_0.1 (dark magenta line) and max_cw_0.05 (light magenta line). The shading color represents the variation of the canopy water between the first quartile and the third quartile from the last eight years of each simulation. (b) The comparison of the diurnal cycle of LH fluxes among CTR, max_cw_0.2 and max_cw_0.1 and max_cw_0.05. The shading color represents the variation of the canopy water between the first quartile and the third quartile from the last eight years of each simulation. (c) The partition of LH flux among CTR, max_cw_0.2 and max_cw_0.1 and max_cw_0.05. The solid lines, dashed lines and dotted lines represent canopy evaporation, transpiration, and ground evaporation, respectively.

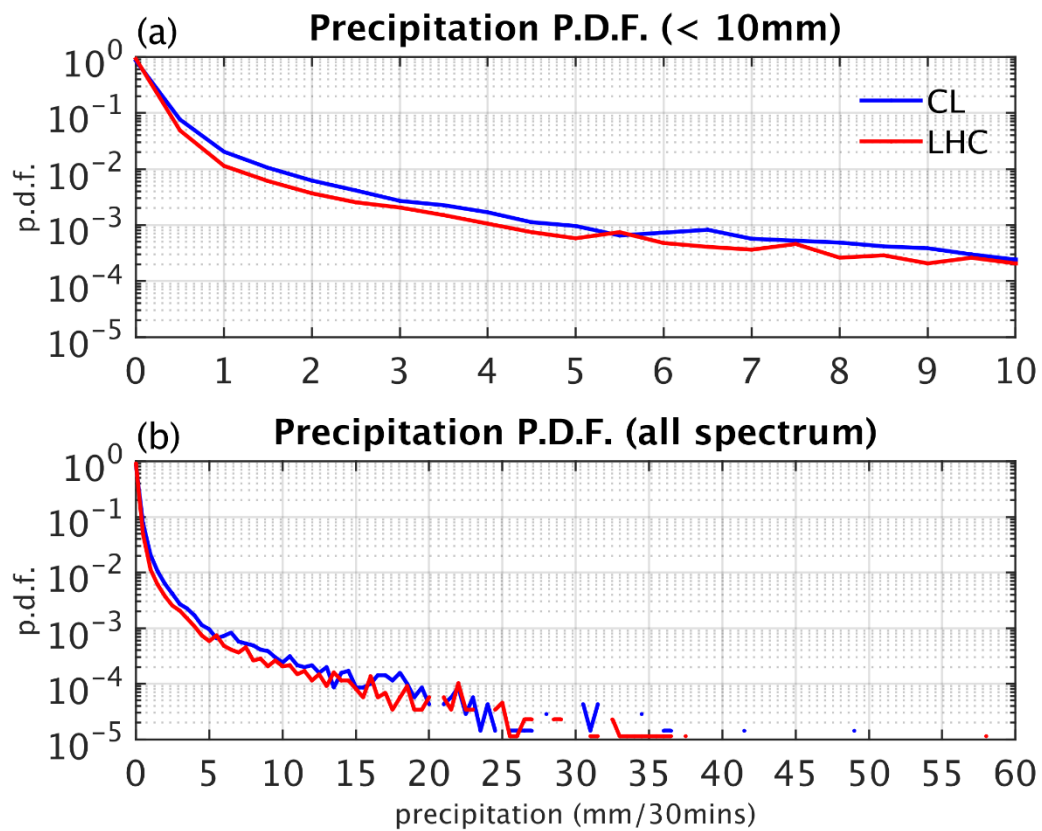


Figure 4.3 The comparison of probability density function (P.D.F.) in precipitation between CL (blue line) and LHC (red line).

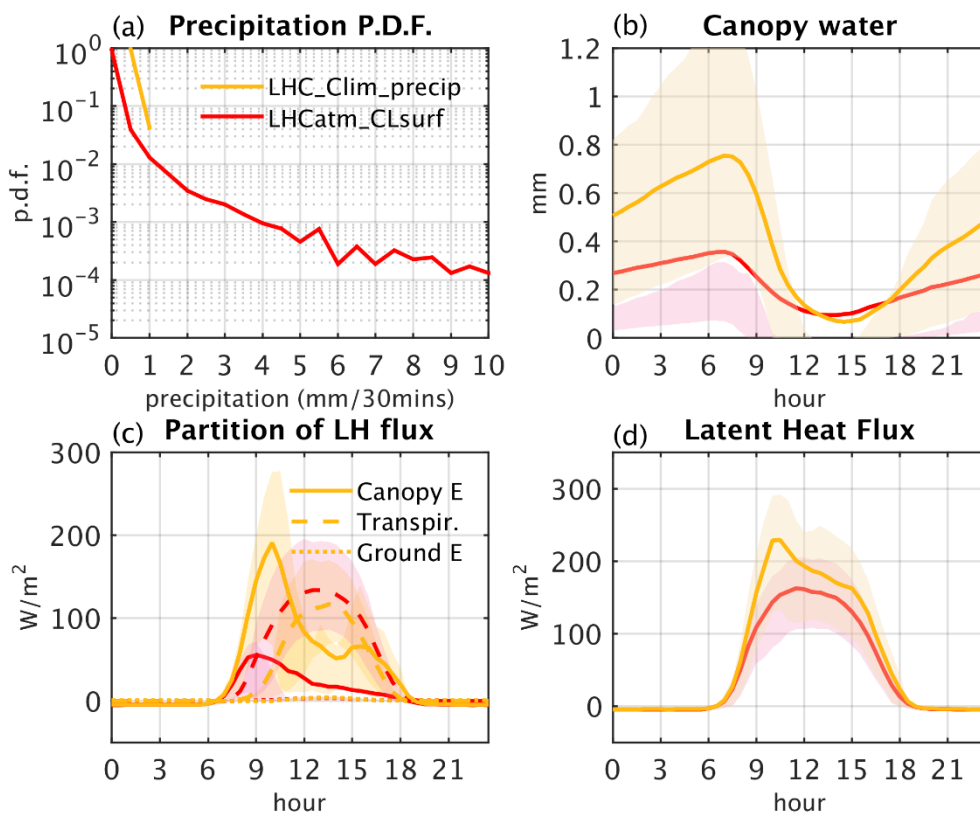


Figure 4.4 (a) The comparison of probability density function in precipitation between LHCatm_CLsurf (red line) and LHCatm_Clim_precip (orange line). (b) The comparison of the diurnal cycle of canopy water among LHCatm_CLsurf and LHCatm_Clim_precip. The shading color represents the variation of the canopy water between the first quartile and the third quartile from the last nine years of each simulation. (c) The partition of LH flux among LHCatm_CLsurf and LHCatm_Clim_precip. The solid lines, dashed lines and dotted lines represent canopy evaporation, transpiration, and ground evaporation, respectively. The shading color represents the variation of the canopy water between the first quartile and the third quartile from the last nine years of each simulation. (d) The comparison of the diurnal cycle of LH flux among LHCatm_CLsurf and LHCatm_Clim_precip. The shading color represents the variation of the LH fluxes between the first quartile and the third quartile from the last nine years of each simulation.

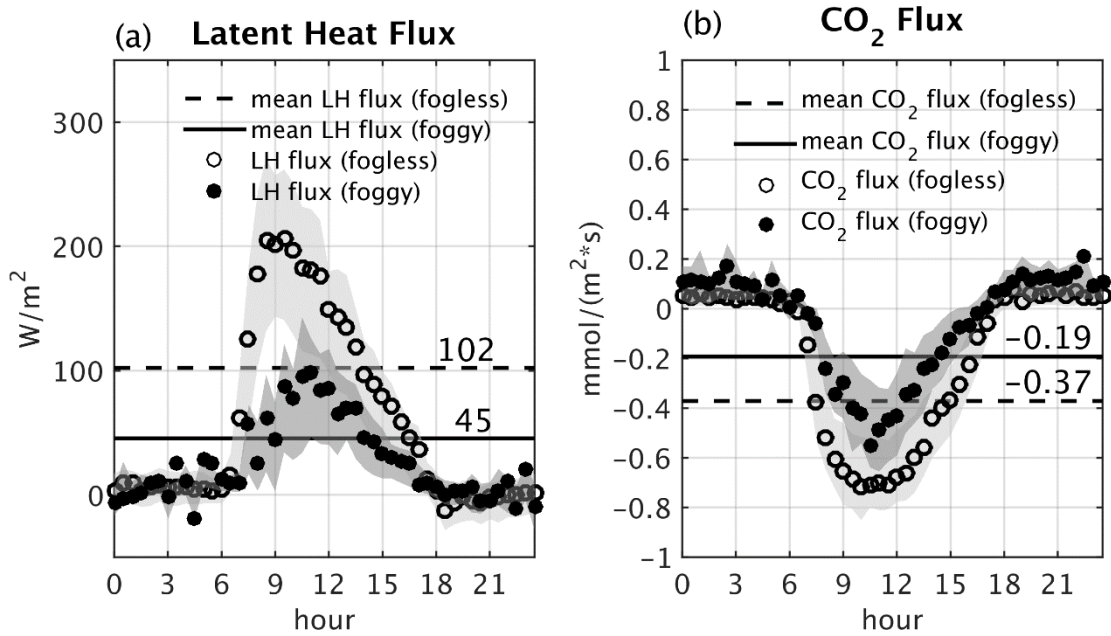


Figure 4.5 The effects of fog on (a) LH flux and (b) CO₂ flux in CL montane cloud-fog forest. The solid dots represent the mean values of fluxes in foggy conditions in each time step, while the hollow dots represent those in fogless conditions. The solid line shows the averaged fluxes in foggy conditions from 6 a.m. to 6:30 p.m., while the dashed line shows those in fogless conditions from 6 a.m. to 6:30 p.m.

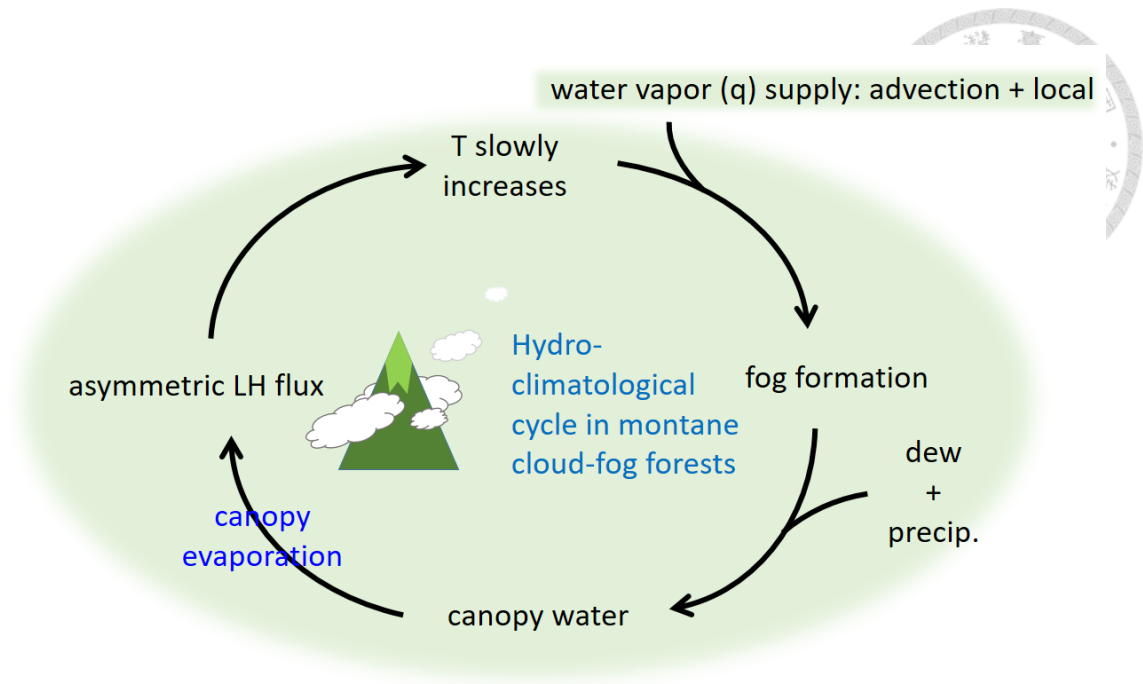


Figure 5.1 Schematic plot of the hydro-climatological cycle in CL montane cloud forest.

TABLES



Table 2.1 Experiment design: the contribution of canopy water on the LH flux

Name of experiments	Land surface condition	Atmospheric forcing (Atm.)	Source of canopy water	Setting details
CTR	CL	CL	precip. dew fog	<p>Land: 100% needleleaf evergreen tree, annual mean LAI = 4.6, coefficient of maximum allowed dew = 0.2533</p> <p>Atm.: CL 2008~2011 half-hourly observational data Precip. is added by 0.2mm per 30 mins when visibility < 1km.</p>
EXP	CL	CL	X	<p>Land: the same as CTR</p> <p>Atm.: the same as CTR Water will drip on the ground as soon as it form or intercept on the canopy.</p>



Table 2.2 Experiment design: canopy water sensitivity test

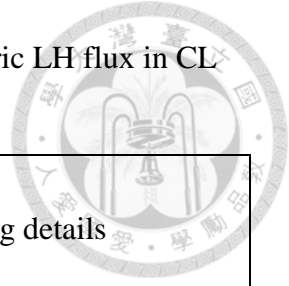
Name of experiments	Land surface condition	Atmospheric forcing (Atm.)	Source of canopy water	Setting details
CTR	CL	CL	precip. dew fog	<p>Land: 100% needleleaf evergreen tree, annual mean LAI = 4.6, coefficient of maximum allowed dew = 0.2533</p> <p>Atm.: CL 2008~2011 half-hourly observational data Precip. is added by 0.2mm per 30 mins when visibility < 1km.</p>
Rain+Dew	CL	CL	precip. dew	<p>Land: the same as CTR</p> <p>Atm.: Precipitation forcing did not include fog as a source of canopy water.</p>
DEWonly	CL	CL	dew	<p>Land: the same as CTR</p> <p>Atm.: the same as CTR Water cannot intercept on the canopy. The interception coefficient is converted from 0.25 to 0.</p>

Table 2.3 Experiment design: the controlling factors to the asymmetric LH flux in CL (group 1)



Name of experiments	Land surface condition	Atmospheric forcing (Atm.)	Source of canopy water	Setting details
CTR_3yr	CL	CL	precip. dew fog	Land: the same as CTR Atm.: CL 2009~2011 half-hourly observational data Precip. is added by 0.2mm per 30 mins when visibility < 1km.
LHCatm_CLsurf	CL	LHC	precip. dew	Land: the same as CTR Atm.: LHC 2009~2011 half-hourly observational data
CLatm_LHCsurf	LHC	CL	precip. dew fog	Land: 42.2% needleleaf evergreen tree, 38.6% broadleaf evergreen tree, 19.2% broadleaf evergreen shrub, annual mean LAI = 3.9519. Atm.: the same as CTR_3yr

Table 2.4 Experiment design: the controlling factors to the asymmetric LH flux in CL (group 2)



Name of experiments	Land surface condition	Atmospheric forcing (Atm.)	Source of canopy water	Setting details
LHCatm_CLsurf	CL	LHC	precip. dew	Land: the same as CTR Atm.: LHC 2009~2011 half-hourly observational data
LHCatm_CL_ws	CL	LHC atm. but CL wind speed	precip. dew	Land: the same as CTR Atm.: the same as LHCatm_CLsurf but using CL wind speed
LHCatm_CL_precip	CL	LHC atm. but CL precipitation	precip. dew fog	Land: the same as CTR Atm.: the same as LHCatm_CLsurf but using CL precipitation
LHCatm_CL_T	CL	LHC atm. but CL temperature	precip. dew	Land: the same as CTR Atm.: the same as LHCatm_CLsurf but using CL temperature
LHCatm_CL_Q	CL	LHC atm. but CL specific humidity	precip. dew	Land: the same as CTR Atm.: the same as LHCatm_CLsurf but using CL specific humidity
LHCatm_CL_P	CL	LHC atm. but CL pressure	precip. dew	Land: the same as CTR Atm.: the same as LHCatm_CLsurf but using CL pressure
LHCatm_CL_SWdw	CL	LHC atm. but CL downward solar radiation	precip. dew	Land: the same as CTR Atm.: the same as LHCatm_CLsurf but

				using CL downward solar radiation
LHCatm_CL_LWdw	CL	LHC atm. but CL downward longwave radiation	precip. dew	Land: the same as CTR Atm.: the same as LHCatm_CLsurf but using CL downward longwave radiation

Table 3.1 The difference of leaf wetness between 6 a.m. and 9 a.m. in 3 different canopy layers. The positive mean value represents the canopy being wetter at 6 a.m. than at 9 a.m.

Height(m)	Difference of leaf wetness between 6 a.m. and 9 a.m. (mean(mV) \pm std)
5.3	32.39 \pm 62.31*
8.3	70.25 \pm 102.44*
11.2	1.87 \pm 26.9
3 layer averaged	36.95 \pm 56.81*
*The value shows significant difference at the 1% significance level, according to one-tailed t test	

Table 4.1 Experiment design: the sensitivity test of the maximum allowed canopy water

Name of experiments	Land surface condition	Atmospheric forcing (Atm.)	Source of canopy water	Setting details
CTR	CL	CL	precip. dew fog	<p>Land: 100% needleleaf evergreen tree, annual mean LAI = 4.6, coefficient of maximum allowed dew = 0.2533</p> <p>Atm.: CL 2008~2011 half-hourly observational data Precip. is added by 0.2mm per 30 mins when visibility < 1km.</p>
max_cw_0.2	CL	CL	precip. dew fog	<p>Land: coefficient of maximum allowed dew = 0.2, the rest of the setting remains the same as CTR</p> <p>Atm.: the same as CTR</p>
max_cw_0.1	CL	CL	precip. dew fog	<p>Land: coefficient of maximum allowed dew = 0.1, the rest of the setting remains the same as CTR</p> <p>Atm.: the same as CTR</p>
max_cw_0.05	CL	CL	precip. dew fog	<p>Land: coefficient of maximum allowed dew = 0.05, the rest of the setting remains the same as CTR</p> <p>Atm.: the same as CTR</p>

Table 4.2 Experiment design: the impact of drizzle on the asymmetry of LH flux

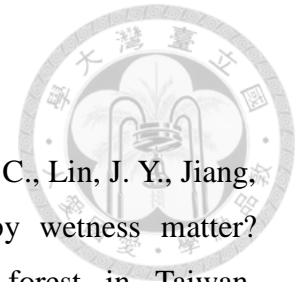
Name of experiments	Land surface condition	Atmospheric forcing (Atm.)	Source of canopy water	Setting details
LHCatm_CLsurf	CL	LHC	precip. dew	Land: the same as CTR Atm.: LHC 2009~2011 half-hourly observational data
LHCatm_Clim_precip	CL	LHC	precip. dew	Land: the same as CTR Atm.: LHC 2009~2011 half-hourly observational data but with repeating climatological diurnal precipitation in every month

REFERENCES



- Anber, U., Gentine, P., Wang, S., & Sobel, A. H. (2015). Fog and rain in the Amazon. *Proceedings of the National Academy of Sciences*, *112*(37), 11473-11477.
- Ataroff, M., & Rada, F. (2000). Deforestation impact on water dynamics in a Venezuelan Andean cloud forest. *AMBIO: A Journal of the Human Environment*, *29*(7), 440-444.
- Bruijnzeel, L., Mulligan, M., & Scatena, F. N. (2011). Hydrometeorology of tropical montane cloud forests: emerging patterns. *Hydrological Processes*, *25*(3), 465-498.
- Bruijnzeel, L. A. (2001). Hydrology of tropical montane cloud forests: a reassessment. *Land use and water resources research*, *1*(1732-2016-140258), 1.1-1.18.
- Bubb, P., May, I. A., Miles, L., & Sayer, J. (2004). Cloud forest agenda.
- Chang, S.-C., Lai, I.-L., & Wu, J.-T. (2002). Estimation of fog deposition on epiphytic bryophytes in a subtropical montane forest ecosystem in northeastern Taiwan. *Atmospheric Research*, *64*(1-4), 159-167.
- Chang, S.-C., Yeh, C.-F., Wu, M.-J., Hsia, Y.-J., & Wu, J.-T. (2006). Quantifying fog water deposition by in situ exposure experiments in a mountainous coniferous forest in Taiwan. *Forest Ecology and Management*, *224*(1-2), 11-18.
- Chen, C.-Y. (2016). Investigating interannual and seasonal variations of energy balance in a mountain cloud forest in Chi-Lan Mountain. *National Taiwan University Master Thesis*
- Chen, Y.-Y., & Li, M.-H. (2012). Determining Adequate Averaging Periods and Reference Coordinates for Eddy Covariance Measurements of Surface Heat and Water Vapor Fluxes over Mountainous Terrain. *Terrestrial, Atmospheric &*

Oceanic Sciences, 23(6).



Chu, H. S., Chang, S. C., Klemm, O., Lai, C. W., Lin, Y. Z., Wu, C. C., Lin, J. Y., Jiang, J. Y., Chen, J., & Gottgens, J. F. (2014). Does canopy wetness matter? Evapotranspiration from a subtropical montane cloud forest in Taiwan. *Hydrological Processes*, 28(3), 1190-1214.

Dawson, T. E., & Goldsmith, G. R. (2018). The value of wet leaves. *New Phytologist*, 219(4), 1156-1169.

Dore, M. H. (2005). Climate change and changes in global precipitation patterns: what do we know? *Environment international*, 31(8), 1167-1181.

Foster, P. (2001). The potential negative impacts of global climate change on tropical montane cloud forests. *Earth-Science Reviews*, 55(1-2), 73-106.

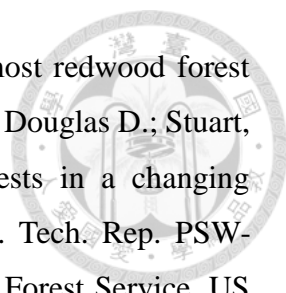
Giambelluca, T. W., Martin, R. E., Asner, G. P., Huang, M., Mudd, R. G., Nullet, M. A., DeLay, J. K., & Foote, D. (2009). Evapotranspiration and energy balance of native wet montane cloud forest in Hawaii 'i. *Agricultural and Forest Meteorology*, 149(2), 230-243.

Goldsmith, G. R., Matzke, N. J., & Dawson, T. E. (2013). The incidence and implications of clouds for cloud forest plant water relations. *Ecology letters*, 16(3), 307-314.

Klemm, O., Chang, S.-C., & Hsia, Y.-J. (2006). Energy fluxes at a subtropical mountain cloud forest. *Forest Ecology and Management*, 224(1-2), 5-10.

Lai, I., Chang, S.-C., Lin, P.-H., Chou, C.-H., & Wu, J.-T. (2006). Climatic characteristics of the subtropical mountainous cloud forest at the Yuanyang Lake long-term ecological research site, Taiwan. *Taiwania*, 51(4), 317-329.

Limm, E., Simonin, K., & Dawson, T. (2012). Foliar uptake of fog in the coast redwood



ecosystem: a novel drought-alleviation strategy shared by most redwood forest plants. In: Standiford, Richard B.; Weller, Theodore J.; Piirto, Douglas D.; Stuart, John D., tech. coords. Proceedings of coast redwood forests in a changing California: A symposium for scientists and managers. Gen. Tech. Rep. PSW-GTR-238. Albany, CA: Pacific Southwest Research Station, Forest Service, US Department of Agriculture. pp. 273-281,

Maneke-Fiegenbaum, F., Klemm, O., Lai, Y.-J., Hung, C.-Y., & Yu, J.-C. (2018). Carbon Exchange between the Atmosphere and a Subtropical Evergreen Mountain Forest in Taiwan. *Advances in Meteorology*, 2018.

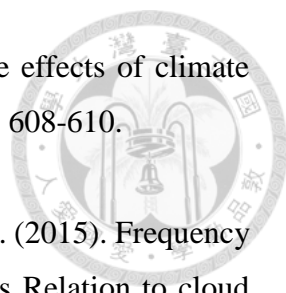
Mildenberger, K., Beiderwieden, E., Hsia, Y.-J., & Klemm, O. (2009). CO₂ and water vapor fluxes above a subtropical mountain cloud forest—The effect of light conditions and fog. *Agricultural and Forest Meteorology*, 149(10), 1730-1736.

Nair, U. S., Lawton, R. O., Welch, R. M., & Pielke Sr, R. (2003). Impact of land use on Costa Rican tropical montane cloud forests: Sensitivity of cumulus cloud field characteristics to lowland deforestation. *Journal of Geophysical Research: Atmospheres*, 108(D7).

Oliveira, R. S., Eller, C. B., Bittencourt, P. R., & Mulligan, M. (2014). The hydroclimatic and ecophysiological basis of cloud forest distributions under current and projected climates. *Annals of botany*, 113(6), 909-920.

Pariyar, S., Chang, S.-C., Zinsmeister, D., Zhou, H., Grantz, D. A., Hunsche, M., & Burkhardt, J. (2017). Xeromorphic traits help to maintain photosynthesis in the perhumid climate of a Taiwanese cloud forest. *Oecologia*, 184(3), 609-621.

Schulz, H. M., Li, C.-F., Thies, B., Chang, S.-C., & Bendix, J. (2017). Mapping the montane cloud forest of Taiwan using 12 year MODIS-derived ground fog frequency data. *PloS one*, 12(2).

- 
- Still, C. J., Foster, P. N., & Schneider, S. H. (1999). Simulating the effects of climate change on tropical montane cloud forests. *Nature*, 398(6728), 608-610.
- Thies, B., Groos, A., Schulz, M., Li, C.-F., Chang, S.-C., & Bendix, J. (2015). Frequency of low clouds in Taiwan retrieved from MODIS data and its Relation to cloud forest occurrence. *Remote Sensing*, 7(10), 12986-13004.
- Wang, A., Zeng, X., Shen, S. S., Zeng, Q.-C., & Dickinson, R. E. (2006). Time scales of land surface hydrology. *Journal of Hydrometeorology*, 7(5), 868-879.
- Wey, T., Lai, Y., Chang, C., Shen, C., Hong, C., Wang, Y., & Chen, M. (2011). Preliminary studies on fog characteristics at Xitou region of central Taiwan. *Journal of the Experimental Forest of National Taiwan University*, 25(2), 149-160.
- Williams, A. P., Schwartz, R. E., Iacobellis, S., Seager, R., Cook, B. I., Still, C. J., Husak, G., & Michaelsen, J. (2015). Urbanization causes increased cloud base height and decreased fog in coastal Southern California. *Geophysical Research Letters*, 42(5), 1527-1536.